# The Dynamic Effects of Renewable Subsidies in the Green Energy Transition *

Tianshi Mu †

November 15, 2023

Click here for the latest version.

**Abstract**

The speed at which electricity generation can transition to green energy sources depends in part on the incentives of coal and natural gas plants to enter or exit. I examine how the design of government subsidies and the costs of renewables shape those strategies. To do so, I formulate a nonstationary dynamic model of generator entry and exit that incorporates heterogeneity in entry costs and nests it within a dynamic, hourly model of competition in the wholesale electricity market. I estimate the model using data from Texas. I find that renewable subsidies in place in 2005–20 reduce cumulative $CO_2$ emissions by 1.71 billion tons though 2060, largely because of a dynamic mechanism: they shift expectations about future competition and thereby reduce the entry of new coal plants very early in the transition. I further show that, by leveraging the dynamic mechanism, a short-horizon subsidy can more effectively reduce carbon emissions with less tax burden by bunching more wind investment and intensifying competition earlier for coal power plants.

**Keywords:** carbon emissions, dynamics, electricity, entry and exit, renewable subsidies, start-up cost, nonstationarity

*I am grateful to my advisors, Nathan Miller and John Rust, as well as Chenyu Yang and Şafak Yücel for their invaluable guidance and support. I thank Cauê Dobbin, Sharat Ganapati, Raphael Calel, Luming Chen, Ming Fang, Jonathan Elliott, Gabriel Weintraub, Gretchen Sileo, and seminar participants at Georgetown University for helpful comments.

†Georgetown University, Department of Economics, 37th and O Streets NW, Washington, DC 20057. Email: tm1323@georgetown.edu. Website: https://tianshimu.netlify.app/.

# 1 Introduction

The green energy transition requires a radical change in the energy sources used to generate electricity. Government subsidies have long been used to encourage earlier and faster expansion of clean energy, such as that derived from wind and solar energy. For example, the US provided $75 billion in tax subsidies over 2005-2020 to support renewables (Kirshenberg 2018;EIA 2023b), and this is projected to reach $220 billion by 2030 under the Inflation Reduction Act (Bistline et al., 2023). Despite the substantial subsidies allocated to green energy, the debate about the duration of these subsidies persists, highlighted by the frequent cycles of expiration and reauthorization before 2015 and the recent commitment in 2022 to extend them for at least 10 years.

This paper studies the design of time horizon for renewable subsidies in a nonstationary environment. The common rationale for these subsidies is to incentivize renewables, enabling economies of scale through learning-by-doing. I deviate from this conventional perspective and explore another mechanism, considering their long-standing nature: they can shape expectations regarding future competition and influence the entry and exit decisions of coal and natural gas generators, even before renewables start to expand. This dynamic mechanism can be leveraged through a careful design of the subsidy horizon to more effectively reduce carbon emissions.

To understand how the subsidies have affected the observed transition path, and how they will affect future outcomes, I develop an annual nonstationary equilibrium model of generator entry and exit that accounts for long-run trends in electricity demand, natural gas prices and renewable installation costs. The model nests a secondary dynamic model of the wholesale electricity market where all generators compete to produce electricity each day during peak and off-peak hours, and coal and natural gas generators are subject to start-up costs. The nested hourly model determines annual profits in the entry and exit model. I estimate the model using data over 2005–20 from Texas. Among estimation results are that the entry costs of coal generators are significantly larger than those of natural gas generators, and that renewables cannibalize more profits from coal than natural gas because of the differences in their characteristics, including fuel costs, operation and maintenance costs and flexibility.

I first use the model to evaluate the effects of a long-standing set of federal renewable subsidies that were in place since 2005 and largely phased out between 2016 and 2020, including the production tax credits (PTCs) and the investment tax credits (ITCs). I find that those subsidies significantly reduce coal entry in the initial years, despite negligible renewable capacities during that period. The subsidies result in a reduction of carbon emissions by 1.7 billion tons through 2060, with 66% of the reduction attributed to the decreased coal expansions. This result highlights the importance of the dynamic mechanism driven by the forward-looking behaviors of coal and natural gas generators. Next, I examine how the duration of the subsidies impacts their performances. I find a nonlinear relationship between the length of the subsidies and their effects on carbon reductions because of bunching in wind investment and the consequent shifts in competition landscape over time. Committing to subsidies with a much shorter horizon can achieve more carbon emissions with less tax burden compared with the one actually implemented between 2005 and 2020.

The paper proceeds as follows. In Section 2, I provide an overview of renewable subsidies in the US and institutional details of electricity market in Texas, and also describe my data sources. The annual data include capacities of different energy sources before 2020, along with statistics about multiple profit shifters, including demand, input prices and engineering estimates of renewable installation costs. The

hourly data include detailed information about electricity demand, electricity prices, generation from wind and solar, fuel costs and outputs from all coal and natural gas generators in 2020. I use the annual data to document the long-term trends in market forces, and use the hourly data to demonstrate the main characteristics of electricity demand and generation from different energy sources. Both long-run trends and those characteristics are important for generator profits; therefore, they inform the following empirical analysis.

I introduce the nonstationary dynamic model in Section 3. I assume that coal and natural gas generators make entry and exit decisions, and that wind and solar generators make entry decisions, all conditional on current and (expected) future demand, costs, and subsidies. Thus, a feature of the model is that generators anticipate and respond to not only future policy changes but also reactions to those future changes from other generators (i.e., equilibrium feedback effects as in Holland et al. (2022)). The model is nonstationary because it incorporates time-varying renewable entry costs (varying due to changes in subsidies and renewable installation costs across years) and profit shifters, which together shape the incentives of generators to enter and exit. One challenge when solving the model is that a curse of dimensionality exists with many generators, as there are in Texas. To reduce the state space for the entry and exit model, I adopt the nonstationary oblivious equilibrium (Benkard et al., 2008) in which generators can make near-optimal decisions by tracking only calendar time $t$ instead of capacities of different types of generators.

Payoffs in the annual model are provided by an hourly model of competition in the wholesale electricity market. The hourly model is also used to evaluate carbon emissions and generation costs under different compositions of coal, natural gas, and renewables along the transition path. I present the hourly model in Section 4. It is important that the hourly model can appropriately reflect the operational characteristics of generators using different energy sources. This is because they determine the competition relationship among energy sources in different hours and result in highly nonlinear profit functions, which are necessary to support the simultaneous entry of ex ante heterogeneous generators in equilibrium.

In the hourly model, I incorporate two aggregate shocks: residual demand (electricity demand net of renewable generation) and natural gas prices. The volatility of these shocks impacts the operation of coal and natural gas generators, which, in turn, determines electricity prices and generator profits. When integrated into the annual model, the distribution of these shocks changes due to long-term trends and variations in renewable capacities, leading to shifts in generator profits.

Turning to the operation of large coal and natural gas generators in the hourly model, I assume that they make two decisions. They first choose whether to operate (start-up decision) subject to start-up costs, a fixed cost incurred when a generator switches from off to on. Then, operating generators choose their output to maximize profits within a constrained range. The literature has identified the substantial impacts of start-up costs on generator profits and how profits would be affected by renewable expansions (Mansur, 2008; Cullen, 2011; Cullen, 2013; Reguant, 2014; Jha and Leslie, 2021; Gowrisankaran et al., 2022). Similarly to previous literature, I model the start-up decisions as dynamic discrete choices. However, aggregate shocks, which are typically simplified in the previous literature, and the large number of generators create another curse of dimensionality, posing difficulties in both solving and estimating the model. Inspired by Gowrisankaran et al. (2022), I reduce the state space by adopting the moment-based equilibrium (Ifrach and Weintraub, 2017) for the hourly model. I assume that generators base start-up decisions on aggregate shocks and only the previous total output from coal and gas generators,

which effectively summarizing the high-dimensional states that those generators would otherwise need to track.

Next, I discuss estimation methods and present estimation results in Section 5. I estimate the hourly model using two steps. First, I estimate the hour-specific distributions of electricity demand, wind and solar utilization factors, and natural gas prices. The estimated distributions replicate the main characteristics of the electricity market, including the hourly cyclical patterns in electricity demand, the intermittency of renewable generation, and the large volatility of natural gas prices. Second, I estimate variable operation and maintenance costs and start-up costs for coal and natural gas generators by the simulated method of moments with equilibrium constraints. It exploits the exogenous variations in renewable generation and input prices, which drive the fluctuations in prices. The estimates deliver a good model fit: the simulation matches well electricity generation and operating frequencies of each type of generators, as well as electricity prices at different hours.

With annual profits from the hourly model, I then calibrate parameters related to generator entry and exit for the annual model, ensuring that coal and natural gas capacity trends align between data and model simulations. The calibration reveals that coal's entry cost per MW is nearly three times greater than that of natural gas. The positive correlation between entry costs and carbon emissions rates drives the entry and exit decisions of coal and natural gas generators and their environmental consequences.

Using the model, I evaluate the impacts of renewable subsidies between 2005 and 2020 in Section 6. I simulate the transition path until 2060 with and without subsidies, and compare the carbon emissions between the two paths. The subsidies reduce carbon emissions by 1.71 billion tons through 2060; however, instead of hastening phase-out of incumbent coal and natural gas generators, 66% of carbon savings come from a reduction of coal expansions by 3.8GW very early in the transition, despite a mere 0.85GW increase in wind during that time. This pattern cannot be explained by a static model. Instead, it arises from a dynamic mechanism: Subsidies that encourage more renewables increase future competition and, consequently, deter the entry of coal. The environmental benefits are achieved with only a minimal reduction in economic surplus. Though subsidies drive an increase in total investment, amounting to $20.1 billion, it is accompanied with a reduction in generation costs by $13.3 billion. The increase in investment arises from the early adoption of renewables, which fails to capitalize on future exogenous cost reductions. The modest decrease in economic surplus implies that these subsidies can effectively operate with a social cost of carbon at just $3.99/ton, significantly lower than recent estimates.

Finally, I examine how subsidies can be better designed in this nonstationary environment to effectively leverage the dynamic mechanism and improve performance. Specifically, I focus on a crucial element of subsidy design: the time horizons. Under alternative horizons, three effects in the transition dynamics stand out. First, the renewable investment tends to cluster in years when the subsidies are about to expire. Second, either early bunching or later but more aggressive expansion of renewables can effectively prevent coal entry. Third, the capacity of natural gas peaks in the middle of energy transition, especially between 2020 and 2030. As a result of the three effects, the analysis shows a nonlinear relationship between the subsidy horizons and the their effects on carbon reductions. Compared with subsidies actually implemented in 2005–20, a shorter-horizon subsidy with only 5 years can more effectively reduce carbon emissions by bunching more wind investment before 2010 and significantly increase competition for coal in the early stage of the transition.

Section 7 concludes the paper and provides directions for future research. Departing from the con-

ventional view on learning effects resulting from renewable subsidies, I illustrate that a less-explored dynamic mechanism—the influence of long-standing subsidies on generators' expectations and their subsequent entry and exit decisions—can have a significant impact on reducing carbon emissions, especially in small markets where the demand for renewable equipment does not inherently drive down renewable costs. Due to the dynamic mechanism and the bunching in renewable investments, a nonlinear relationship exists between subsidy durations and their effectiveness in reducing carbon emissions. This partially elucidates the challenges faced by policymakers in establishing appropriate policy horizons. Despite focusing on small markets, the insights are still important because there are many small countries or regional system operators within a country that can benefit from cost reductions achieved by scale economy elsewhere and better design their own local subsidies.

## 1.1 Related Literature

I contribute to a literature that examines the dynamic effects of climate policies in the electricity market (Linn and McCormack (2019); Gowrisankaran et al., 2023; Eisenberg, 2020; Abito, 2020; Gowrisankaran et al., 2022; Gonzales et al., 2023; Johnston et al., 2022; Elliott, 2022; Holland et al., 2022; Stock and Stuart, 2021; Gillingham et al., 2021; Palmer et al., 2011; Borenstein and Kellogg, 2023), and more broadly in heavy-polluting industries (for example, Ryan, 2012 and Fowlie et al., 2016). The two papers that are closest to mine are Gowrisankaran et al. (2022) and Elliott (2022), both of which examine the impacts of environmental policies on generator entry and exit in a nonstationary environment. Gowrisankaran et al. (2022) study how uncertainty surrounding the Mercury and Air Toxics Standard (MATS), a policy mainly targeting polluting coal power plants, affects their technology adoption and exit of them. The time horizon of subsidies has similar effects to policy uncertainty, as it shifts the power plants' expectations. In my paper, instead of focusing on only one energy source, I study the equilibrium responses to the subsidies from not only wind and solar but coal and natural gas, which are the main sources of carbon emissions. Elliott (2022) studies the impacts of environmental regulation on the electricity market, focusing on the balance between reducing carbon emissions and enhancing reliability. Elliott does not consider coal and natural gas generators' dynamic decisions, which depend on start-up costs, partly because generators in the market he studies are relatively small. In this paper, these dynamics are explicitly modeled in the nested hourly model so that the model better reflects how much large generators in Texas respond to renewable expansions.

The hourly model builds on an extensive literature studying competition in the wholesale electricity market and the role of start-up costs (Borenstein et al., 2002; Bushnell et al., 2008; Wolak, 2007; Reguant, 2014; Gowrisankaran et al., 2016; Mansur, 2008; Fowlie, 2010; Cullen, 2011; Reguant, 2014; Jha and Leslie, 2021). I extend the literature by incorporating aggregate shocks including demand and input prices, and incorporating the effects of energy storage, following Karaduman (2020), so that the hourly model is rich enough to reflect how profits change along the entire transition path. My paper also relates to the literature that employs either the competition models or reduced-form methods to examine the short-run impacts of renewable expansions on carbon emissions and market operations (Kaffine et al., 2013; Novan, 2015; Bushnell and Novan, 2021; Fell and Kaffine, 2018; Jha and Leslie, 2021; Gowrisankaran et al., 2016; Karaduman, 2021; Cullen, 2011). This paper contributes to the literature by modelling dynamics to demonstrate that the sustained presence of subsidies can cause those impacts even before renewable expansion starts. Also, this paper examines those impacts not only in a short period but along the entire transition path.

Finally, in both the annual model and the hourly model, I build on the recent literature approximating Market perfect equilibrium using oblivious strategies (Weintraub et al., 2008;Weintraub et al., 2010;Benkard et al., 2008;Ifrach and Weintraub, 2017) to overcome the curse of dimensionality due to a large number of generators. I apply the nonstationary oblivious equilibrium (Benkard, 2004) to the annual model and employ the moment-based equilibrium (Ifrach and Weintraub, 2017) in the hourly model.[1] This provides a tractable framework for examining issues in a market with many firms, where both long-run decisions and short-run decisions have dynamic considerations.

# 2 Institutional Details and Data

## 2.1 Renewable Subsidies in the US

In this section, I describe renewable subsidies between 2005 and 2020, and the extension of renewable subsidies in the Inflation Reduction Act of 2022. To quickly reduce carbon emissions, significant renewable subsidies were established to encourage earlier adoption of renewable energy sources, including wind and solar. The main subsidies considered in this paper PTCs and ITCs.[2] The ITC is primarily qualified by solar projects and is calculated as a percentage of a project's investment cost. Before 2020, the ITC was 30%, but it was reduced in 2020 and 2021. The PTC, typically applicable to wind projects, is given annually and available for 10 years, in an amount equal to a specified credit rate multiplied by the amount of electricity generated. The credit rates (2020 dollars) before 2022 are plotted in Figure 2a. They remained constant before 2017 and were gradually reduced until 2021. I convert PTC into a lump-sum payment, similar to the ITC.[3] To achieve the goal of zero emissions, the Inflation Reduction Act of 2022 extended renewable subsidies for at least 10 years at a rate of $24.8 for the PTC and at 30% of installation costs for the ITC. They will be phased out either in 2032 or when carbon emissions in the power sector reach 25% of their 2022 levels, whichever comes later.

## 2.2 ERCOT Market

The Electric Reliability Council of Texas (ERCOT) is an independent system operator that manages the majority of the electricity grid in Texas. It schedules electricity flow on a grid that connects 46,500 miles of transmission lines and serves more than 26 million customers. In 2020, 45.5% of electricity generation in ERCOT came from natural gas, 22.8% from wind, 17.9% from coal, 10.9% from nuclear, and 2.9% from other sources including solar, hydro and petroleum coke. Residential consumption accounts for

[1] Both nonstationary oblivious equilibrium and moment-based equilibrium are widely used equilibrium concepts in the literature. Recent applications of nonstationary oblivious equilibrium include Caoui (2023) and Johnston et al. (2022). Recent applications of moment-based equilibrium include Jeon (2022), Vreugdenhil (2020), Gerarden (2023), and Gowrisankaran et al. (2022). Gowrisankaran et al. (2022) extend it to approximate belief oligopoly equilibrium by allowing firms to recognize the impacts of their actions on a reduced set of market states.

[2] Beyond tax credits, renewable portfolio standards (RPS) provide an additional incentive for adopting renewable capacity. RPS requires that a specified percentage of the electricity suppliers sell comes from renewable resources. Texas first adopted an RPS in 1999; it required the state to install 5 GW of new renewable energy capacity by 2015 and set a target of 10 GW of renewable energy capacity by 2025. However, the RPS was not binding because Texas had already reached its 2025 goal in 2009; therefore, I do not consider RPS in this paper.

[3] For example, assume that PTC is $24/MWh and the utilization factor of a wind project is 40%. Then the PTC for 1GW of wind capacity is $84.10 million per year. The equivalent lump-sum payment, assuming that the PTC will last for 10 years, is therefore $841 million.

51.3% of electricity demand in ERCOT, while the commercial sector represents 30.9%, and the industrial sector the remaining 17.8%.

Multiple institutional features of ERCOT inform the empirical analysis. First, ERCOT separates itself from Eastern and Western interconnections as shown in Figure A-1. This isolation makes it unnecessary to include imports and exports in the analysis.

Second, the majority of generators in ERCOT are deregulated.[4] Regulated generators are subject to cost-of-return regulation (Abito, 2020) and operate in accordance with rates established by regulatory authorities, rather than being responsive to wholesale prices. Deregulated generators and regulated generators also differ in their incentives regarding when to retire their capacity(Gowrisankaran et al., 2023).[5]

Third, there is no capacity market in ERCOT. A capacity market provides a subsidy for installed capacity, and the subsidy does not depend on energy production. It is designed to guarantee a sufficient reserve capacity to meet peak demand and prevent blackouts(Fabra, 2018). In the absence of capacity market payments, the sole incentive for market entry is the profits generated from producing and selling electricity.

Fourth, market concentration in ERCOT is very low. In 2020, there were 58 utilities and Herfindahl-Hirschman Index at the utility level was 360. Consequently, the exercise of market power is limited during most hours throughout the year, as evidenced by the significantly lower prices in comparison to other regions. Large utilities often strategically hold off some generators to reduce output and increase prices. Since there is no evidence of high market power, I do not consider the ownership linkage across generators.

## 2.3 Data

The data contain an annual component for the entry and exit model, and an hourly component for the wholesale competition model. The dataset is compiled from various sources, all publicly available.

The primary dataset used for the hourly model is the Continuous Emissions Monitoring System (CEMS) database from the Environmental Protection Agency. It includes hourly electricity generation (MWh), heat input (MMBtu) and carbon emissions (tons) for almost all thermal generators in the US. I screen out generators in Texas but not covered by ERCOT according to their county. Based on CEMS data, I construct several important characteristics of generators. I define the capacity of a generator as the 95th percentile of its hourly output between 2005 and 2020; and similarly to Gowrisankaran et al. (2022), I define a generator's minimum output requirement as the modal generation level in hours when output is in between the generator's 5th and 25th percentiles throughout the sample. The heat rate (MMBtu/MWh) is constructed as the ratio of annual total heat input to total output, and the $CO_2$ emission rate (tons/MWh) is the average mass of carbon divided by hourly output. The remaining characteristics, including primary energy source and technology, come from EIA form 860. [6]

[4] 86% of coal and natural gas generators in my sample are owned by investor-owned utilities.

[5] Gowrisankaran et al. (2023) show that the speed of coal generators' retirement is slower in regulated states because utilities in regulated markets are authorized to charge sufficient rates to recover investment under "used and useful" principal, which requires generators to be physically used and useful to ratepayers even if it is not efficient to use them.

[6] The capacity and minimum output requirement for generators are also provided in EIA form 860; however, it is not a one to one mapping between a unit in CEMS and a generator in EIA (Huetteman et al., 2021). Since the main analysis is at unit level using CEMS data, I do not use capacity and minimum output requirement information

Next, I combine the primary dataset with data about fuel costs. For deregulated power plants, plant-level input prices are not available in EIA. So I apply average input prices in Texas to all generators. I collect daily natural gas prices ($/MMBtu) from Henry Hub, and annual average coal prices in Texas from EIA.

I then merge in wholesale electricity prices, electricity demand, and wind and solar generation, all at the hourly level. I collect day-ahead wholesale electricity prices for each hour in multiple zones from Energy Online[7] and take the average across zones. Electricity load, wind output, and solar output are from the ERCOT website. The hourly utilization factors of wind and solar are calculated as the ratio of output to annual capacity.

Finally, the annual capacities of coal, natural gas, wind, and solar between 2010 and 2020 are aggregated from EIA-860. The wind and solar capacity-expansion forecasts are from Department of Energy and Asmelash and Prakash (2019) respectively. The installation costs of wind and solar between 2013 and 2020 are reported by EIA, and the forecasts in 2030 and 2050 are provided by Irena (2019) and Olson and Bakken (2019) respectively.

## 2.4 Data Description

**Energy Transition in ERCOT** Figure 1 shows annual capacities of the main energy sources for electricity generation in ERCOT. The most remarkable change in the fuel mix is the expansion of renewables. Wind capacity started to increase in 2005 and has accelerated since 2014.[8] Solar capacity began to grow in 2018 and increased by 10 GW within four years. Regarding fossil fuel generators, ERCOT exhibited a steady increase of natural gas capacity.[9] There was an increase in coal capacity between 2005 and 2015. The Clean Power Plan essentially forbid the establishment of new coal generators after 2015 and coal generators started to retire. Nuclear and hydro power account for a small share of electricity generation in ERCOT, and they remain stable over time. Therefore, I assume that the capacity of nuclear and hydro power will remain the same in the future.

in EIA 860.

[7] `http://www.energyonline.com/Data/GenericData.aspx?DataId=23&ERCOT___Day-Ahead_Price`

[8] I consider on-shore wind only. In 2020, only 2% of wind capacity came from off-shore wind farms, and their share is projected by US Department of Energy to increase to only 4% in 2050 (Department of Energy, 2023).

[9] There are mainly three technologies for natural gas generators in ERCOT: combined-cycle gas turbine, open-cycle gas turbine, and steam turbine. I focus on combined-cycle gas turbines because they account for the majority of natural gas generators in ERCOT.

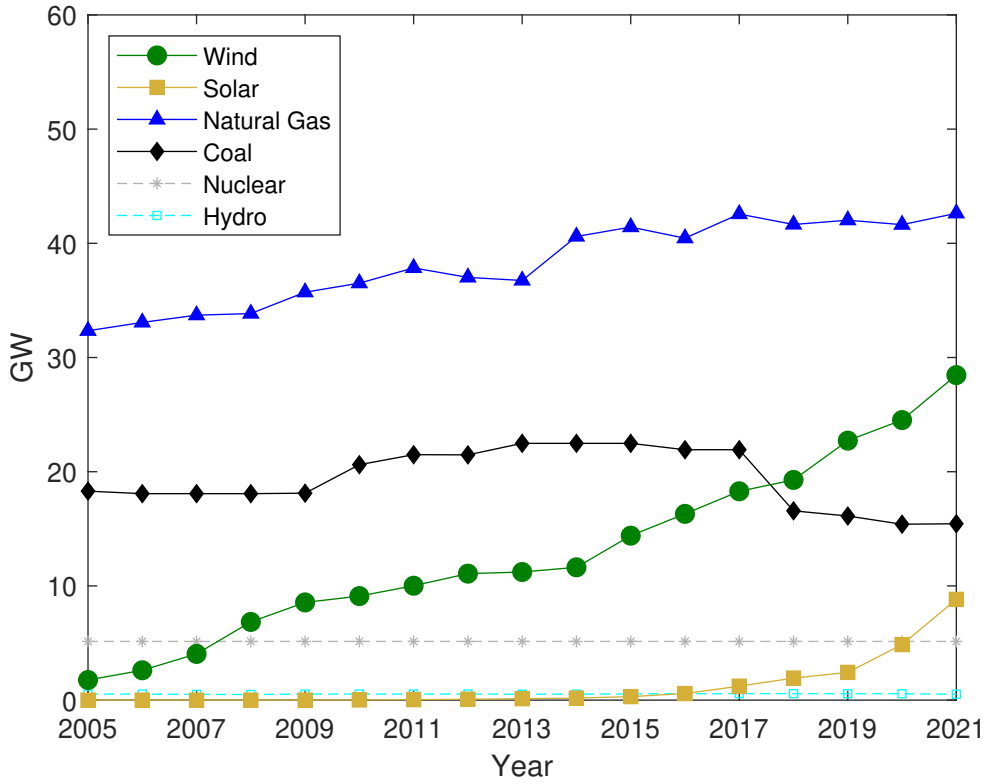


Figure 1: Capacity by Primary Energy Source

*Notes*: I calculate capacity by primary energy source using data from EIA 860. Generators that temporarily disappear in EIA 860 are assumed to continue operating in gap years.

**Contemporary Trends** Besides renewable subsidies, multiple other trends contribute to the changes in ERCOT's fuel mix. First, the installation costs of wind and solar fell sharply between 2005 and 2020, and they are projected to fall even further. The main driving forces of the cost reduction are R&D and learning by doing (Rubin et al., 2015;Bollinger and Gillingham, 2019;Covert and Sweeney, 2022). Since demand for wind turbines and solar photovoltaic from ERCOT accounts for a tiny share of global production, I assume the decline in installation costs is exogenous. Another technology advancement comes from the shale gas revolution. The combination of hydraulic fracturing and horizontal drilling significantly increased the production of natural gas and reduced the natural gas price from \$9.4/MMBtu to \$2.0/MMBtu between 2005 and 2020, as shown in Figure 2d.[10] The price of coal is stable over time because most power plants and coal mines are vertically integrated and prices are determined by long-term contracts. Finally, electricity demand has been increasing since 2005 because of continued population growth in Texas, and demand in peak hours and off-peak hours has increased in parallel.

[10]The natural gas price jumped to \$7.5/MMBtu in 2022 temporarily because of production freeze-offs in the first quarter and high net withdrawals from storage, but it returned to \$4/MMBtu in October(EIA, 2023a).

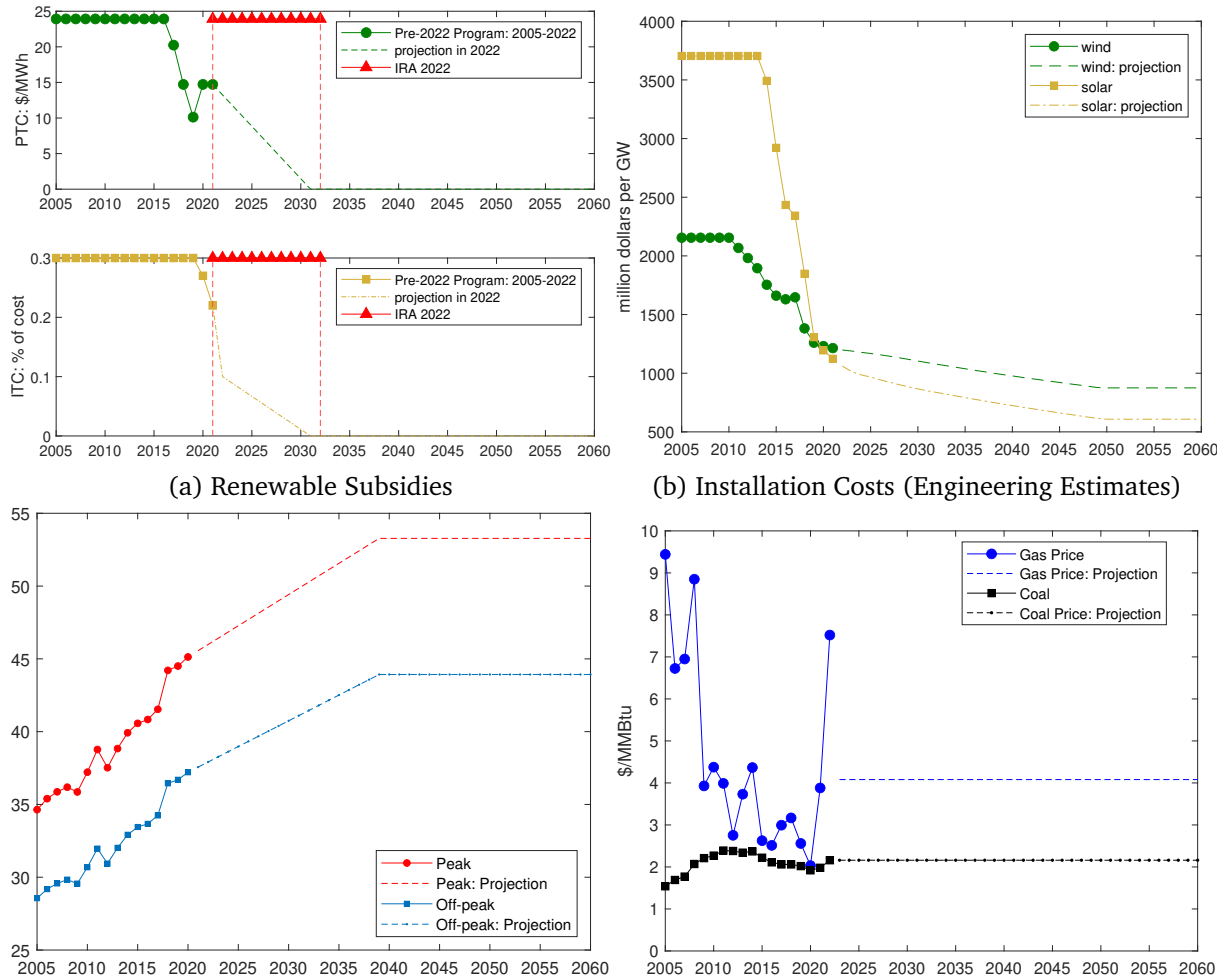


(a) Renewable Subsidies

(b) Installation Costs (Engineering Estimates)

(c) Electricity Demand

(d) Input Prices

Figure 2: Contemporary Trends and Projections

*Notes*: **Panel (a)** shows historical rates of PTCs for wind projects and ITCs for solar projects between 2005 and 2020. Absent the Inflation Reduction Act, I assume that both PTCs and ITCs would have gradually phased out. IRA 2022 extended both subsidies by at least 10 years(Bistline et al., 2023). In the empirical analysis, the PTC is converted into a lump-sum payment as an ITC, on the assumption that the utilization factors of wind will remain the same in the next 10 years.

**Panel (b)** shows engineering estimates of installation costs for on-shore wind and solar panels. Data between 2010 and 2020 come from EIA, and they are assumed to be constant before 2010. Installation costs for utility-scale solar are projected to decrease by 50% by 2050 compared with 2020 (Olson and Bakken, 2019). For wind, I follow Irena (2019), who estimates that installation costs of on-shore wind will be \$0.8–\$1.35 million/MW in 2030 and \$0.6-\$1 million/MW in 2050. I use the midpoints of these intervals and linearly interpolate the installation costs between 2020 and 2030 and between 2030 and 2050.

**Panel (c)** plots the annual averages of electricity demand in peak hours and off-peak hours. Before 2022, they are calculated from hourly load data in each year. I project future demand according to the business-as-usual case in Choukulkar (2022) except that I assume that demand remains constant after 2040.

**Panel (d)** plots annual averages of natural gas prices and coal prices. Natural gas prices before 2022 are calculated from daily Henry Hub natural prices, and coal prices in Texas come from EIA. I assume that natural gas prices will remain at \$4.08/MMBtu after 2022.

**Hourly Wholesale Electricity Market** Electricity is distinct from other commodities because of multiple unique characteristics of its demand and supply. These attributes play a crucial role in shaping generators' profits under alternative fuel mixes, and they therefore determine the incentives for entry and exit in the long run.

First, electricity demand is inelastic with respect to electricity prices.[11] Second, demand varies cyclically over the course of a day as illustrated in Figure 3a, which displays the mean and 5th–95th percentiles of electricity demand by hour in 2020. Electricity demand typically peaks between 1 p.m. and 8 p.m. and plummets at night and in the early morning. Peak hours also exhibit larger variation across days than off-peak hours. Third, given capacity, wind and solar generation are exogenous, contingent upon the intensity of wind and sunlight. Figure 3c plots the mean and 5th–95th percentiles of utilization factors for wind and solar. Comparing that figure with Figure 3a illustrates the intermittency of renewable generation. Wind generation cannot rise when demand peaks and solar generation is limited to daytime. Additionally, the variability in wind and solar generation across days amplifies the fluctuations in residual demand (demand net of renewable generation) faced by coal and natural gas generators.

Each hour, coal and natural gas generators make two types of decisions. First, they decide whether to operate, taking into account the start-up cost, a fixed cost incurred when a generator switches from being idle to producing any positive amount. This fixed cost includes substantial fuel costs and opportunity costs arising from potential boiler-equipment damages. Figure 3b plots the probability of operating by hour of the day for coal and natural gas separately. More than 80% of coal generators and about 60% of natural gas generators choose to be on at night, when electricity prices are even lower than fuel costs. This suggests that both coal and natural gas generators are subject to significant startup costs. However, compared with peak hours, at night 20% less natural gas and almost no coal is idle. This suggests that natural gas generators have much smaller start-up costs than coal generators. Second, conditional on operating, coal and natural gas generators decide how much to produce with an increasing marginal cost curve and suject to a limited range of output levels. The maximum output of a generator is constrained by capacity, which is determined at the time of construction and remains fixed over time. The minimum output requirement sets a lower bound for output; Producing below it results in inefficiency and equipment damages. Figure 3d plots the utilization factors of coal and natural gas generators when they are on. As prices rise from \$15/MWh at 5 a.m. to \$55/MWh at 5 p.m., the utilization factor of coal increases from 50% to 80%, about two times the response from natural gas generators. This suggests a steeper marginal cost curve for coal than natural gas.

[11] Absent smart metering and real-time pricing, very few consumers are willing and able to adjust their consumption to price fluctuations in the wholesale market.

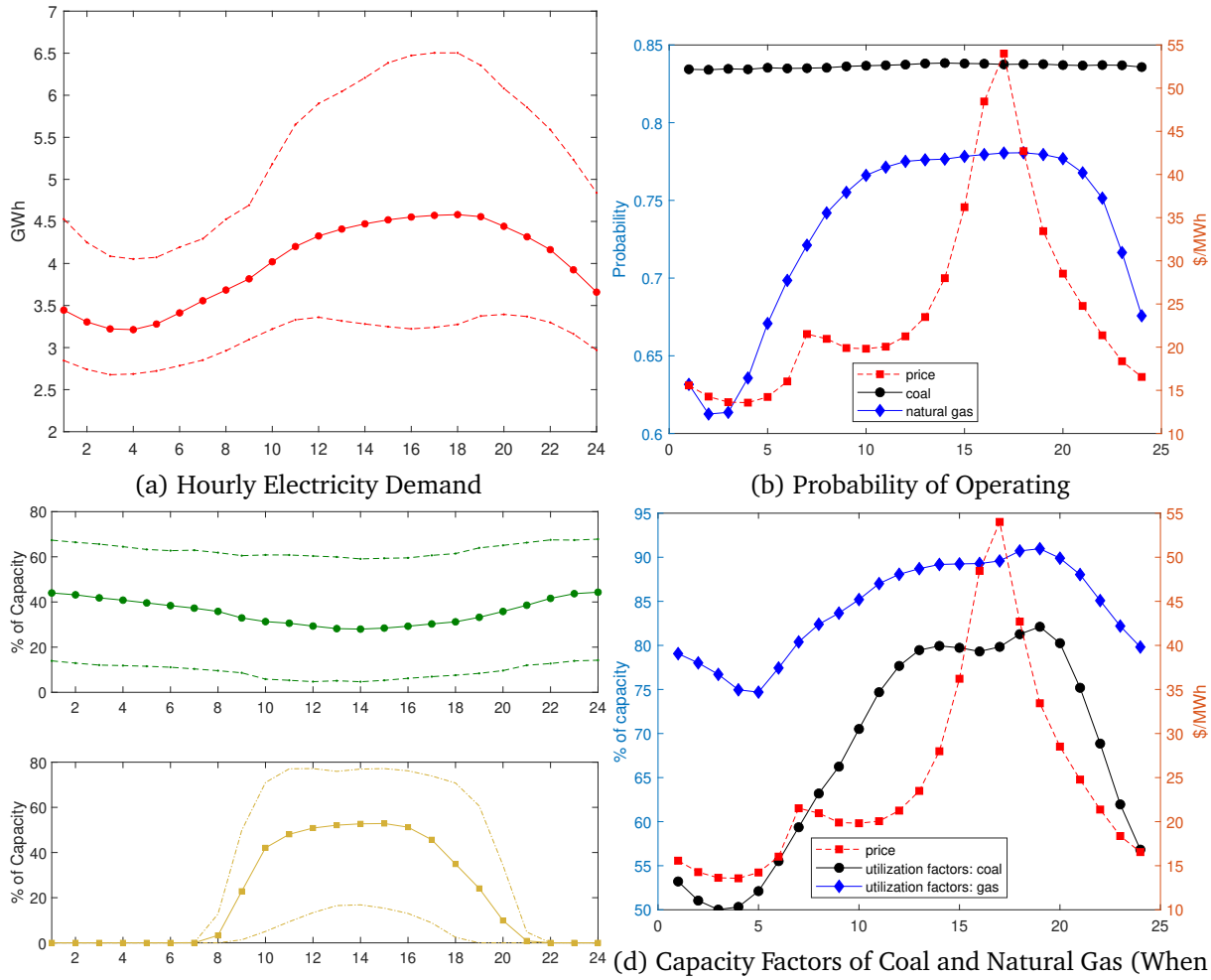


(a) Hourly Electricity Demand

(b) Probability of Operating

(c) Capacity Factors of Wind and Solar

(d) Capacity Factors of Coal and Natural Gas (When Operational)

Figure 3: Operation Characteristics of the Hourly Electricity Market

*Notes*: All panels use data from ERCOT in 2020.
**Panel (a)** shows the mean and 5th–95th percentiles of electricity demand by hour of day.
**Panel (b)** shows mean electricity prices by hour of day and the operation probabilities for coal and natural gas generators.
**Panel (c)** shows the mean and 5th–95th percentiles of capacity factors by hour of day for wind (upper panel) and solar (lower panel).
**Panel (d)** shows mean electricity prices by hour of day and utilization factors conditional on operation for coal and natural gas generators.

I categorize generators into two groups: dominant and fringe. I model the operation of individual dominant generators in greater detail, including their dynamic start-up decisions and output decisions. As for the fringe generators, I group all of them as a representative subject. It makes a single static output decision, subject to an increasing marginal cost curve, without start-up costs or output constraints. The distinction between dominant and fringe generators is based on their sizes and operation frequencies. Smaller generators, which have significantly lower start-up costs, and generators that operate only during a very short period in a year, are not considered for dynamic decisions. Specifically, a generator is considered dominant if it meets two criteria: (1) capacity exceeds 100 MW and (2) it operated for

more than 60% of all hours in at least one year between 2005 and 2020. In 2020, dominant generators constituted 80% of all coal and natural gas generators.

Table 1 provides summary statistics of the dominant generators. I consider three types of generators: coal, small natural gas, and large natural gas. I assume there is no heterogeneity within each type and use the mean as the representative attribute for each type. Coal generators have considerably larger capacity than natural gas generators. Minimum output accounts for a substantial portion of the capacity: 42% for coal generators, 66% for small gas generators and 54% for large gas generators. Natural gas generators are typically more fuel efficient than coal generators, as measured by heat rates. Carbon emission rates from natural gas generators are about half of coal generators' rates, which implies that replacing coal with natural gas will benefit the environment. However, since natural gas generators still produce substantial carbon emissions compared with renewables, it is desirable to gradually phase them out.

Table 1: Summary Statistics of Dominant Generators

| | Coal | Natural Gas: Small | Natural Gas: Large |
|---|---|---|---|
| Capacity (MW) | 741.63 | 252.06 | 421.29 |
| | (163.05) | (51.08) | (100.82) |
| Minimum Output Requirement (MW) | 313.00 | 167.26 | 228.50 |
| | (123.26) | (40.08) | (14.57) |
| Heat Rate (MMBtu/MWh) | 9.89 | 7.58 | 6.98 |
| | (0.69) | (1.38) | (0.45) |
| $CO_2$ Emission Rate (tons/MWh) | 1.06 | 0.47 | 0.44 |
| | (0.06) | (0.08) | (0.04) |
| N | 19 | 78 | 14 |

***Notes***: The table provides summary statistics of coal and natural gas generators whose capacity is larger than 100MW and who operate in more than 60% of the hours in at least one year between 2005 and 2020. Natural gas generators are further categorized as small or large based on whether their capacity is less than 300MW. Characteristics of generators are calculated based on Continuous Emissions Monitoring System data (see Section 2.3).

# 3 Annual Entry and Exit Model

In this section, I present the annual nonstationary dynamic model of generator entry and exit. I employ the model to simulate the transition paths — that is, capacities of different energy sources under different policy scenarios.

Time is discrete with infinite horizon $t = 0, 1, 2, \cdots$. I assume that there exists a terminal period $\overline{T}$ after which all coal and natural gas generators are forced to exit and there is no further entry of wind and solar. In other words, the market remains in a steady state after $\overline{T}$.

There are five types of generators $j \in \mathcal{J} = \{$coal, small natural gas, large natural gas, wind, and solar$\}$, and generators within each type are homogeneous and indexed by $i$. Generators make independent entry and exit decisions. Period profit of a generator with type $j$ is determined by a deterministic function $\pi(K_t, z_t)$, where $K_t = (K_t^{\text{coal}}, K_t^{\text{small gas}}, K_t^{\text{large gas}}, K_t^{\text{wind}}, K_t^{\text{solar}})$ represents the incumbent capacity of each energy source and $z_t = (z_t^d, z_t^g, z_t^b)$ are profit shifters associated with electricity demand, natural gas prices, and the effects of energy storage. The profit function is microfounded in the hourly competi-

tion model, which is introduced in the next section. $\{K_t\}_{t=0}^{\infty}$ is endogenously determined by generator entry and exit, and I assume that generators have perfect foresight about $\{z_t\}_{t=0}^{\infty}$.

The timeline before period $\overline{T}$ is as follows:

- Incumbents and potential entrants observe market state $(K_t, t)$. Incumbent coal or natural gas generators also privately observe independent scrap value $\phi_{it}^j \sim F^{\phi,j}$.
- Each generator forms expectations over the evolution of future $K_t$.
- Based on current period profits, future profit shifters, and expectations about future capacity of each energy source, incumbent coal and natural gas generators decide whether to exit. Incumbent wind and solar generators never exit the market. Potential entrants of all types decide whether to enter the market. If they enter, coal and natural gas generators pay fixed entry costs $\psi^j, j \in \{\text{coal, small natural gas, large natural gas}\}$, and the entry costs associated with wind and solar are time varying and calculated as installation costs $I_t^j$ net of subsidies $\Gamma_t^j$, $\psi_t^j = I_t^j - \Gamma_t^j, j \in \{\text{wind, solar}\}$.
- Finally, each generator acts on its entry/exit decision and $K_t$ evolves accordingly.

Calendar time $t$ plays an important role in the model. First, profit shifters exhibit long-run trends. Second, the installation costs are declining over time. Third, the renewable subsidies are time dependent. Generators keep track of $(K_t, t)$ in the Markov perfect equilibrium (MPE). It is a six-dimension object and therefore imposes a curse of dimensionality. To reduce the state space in this nonstationary environment, instead of MPE, I adopt non-stationary oblivious equilibrium as proposed by Benkard et al. (2008). It exploits the fact that when there are many generators, for each type, the effects on total capacity from individual-generator entry and exit almost wash out. Therefore, when coupled with the assumption that generators are infinitesimal,[12] capacity of each energy sources follows roughly a deterministic trajectory. Specifically, suppose that generators of type $j$ use common strategy $\zeta_t^j(K_t, z_t)$, which represents the probability of exit in period $t$, and there are new entrants of mass $\lambda_t^j(K_t, z_t)$. Then the expected capacity of each energy source follows

$$\begin{aligned}
\widetilde{K}_t^{coal} &= \widetilde{K}_{t-1}^{coal}(1-\zeta_t^{coal}) + \lambda_t^{coal} \\
\widetilde{K}_t^{gas:small} &= \widetilde{K}_{t-1}^{gas:small}(1-\zeta_t^{gas:small}) + \lambda_t^{gas:small} \\
\widetilde{K}_t^{gas:large} &= \widetilde{K}_{t-1}^{gas:large}(1-\zeta_t^{gas:large}) + \lambda_t^{gas:large} \\
\widetilde{K}_t^{wind} &= \widetilde{K}_{t-1}^{wind} + \lambda_t^{wind} \\
\widetilde{K}_t^{solar} &= \widetilde{K}_{t-1}^{solar} + \lambda_t^{solar},
\end{aligned} \tag{1}$$

with $\widetilde{K}_0^i = K_0^i$. Instead of tracking $(K_t, t)$ and forming expectations about $K_t$, generators can approximate future profits using $\widetilde{K}_t$ and therefore make near-optimal decisions by tracking only calendar time $t$.

The following Bellman equation characterizes the dynamic programming problem of an incumbent coal or natural gas generator:

[12] I assume generators are infinitesimal to avoid the integer problem in the state transition process, similarly to Cullen and Reynolds (2023).

$$V_t^i(\phi_{it}^j) = \Pi_t^{j(i)}(\widetilde{K}_t, z_t) + \max\{\phi_{it}^j, \beta E[V_{t+1}^i(\phi_{it+1}^j)]\}. \tag{2}$$

The ex ante value function (before the realization of $\phi_{it}^j$), $V_t^j$, is given by

$$V_t^j = \Pi_t^j(\widetilde{K}_t, z_t) + \zeta_t^j E[\phi_{it}^j | \phi_{it}^j \geq \beta V_{t+1}^j] + (1 - \zeta_t^j)\beta E V_{t+1}^j,$$

where $\zeta_t^j = E[\mathcal{I}\{\phi_{it}^j \geq \beta V_{t+1}^j\}]$ represents the probability of exit in period $t$, with $\mathcal{I}\{\cdot\}$ being an indicator function. I further assume that scrap values follow independent exponential distributions with mean $\overline{\phi}^j$. Then,

$$\zeta_t^j = \exp\{-\frac{\beta V_{t+1}^j}{\overline{\phi}^j}\}$$

and

$$E[\phi_{it}^j | \phi_{it}^j \geq \beta V_{t+1}^j] = \overline{\phi}^j + \beta V_{t+1}^j.$$

I assume that there is a large pool of potential entrants for each energy source. If each potential entrant plays a symmetric mixed entry strategy, following Weintraub et al. (2008), the capacity of new entrants is approximated by the Poisson distribution with a state-dependent mean, $\lambda_t^j$, which is determined by free-entry conditions. Specifically,

$$\begin{aligned} &\psi_t^j \leq \beta V_{t+1}^j \text{ implies } \lambda_t^j = \overline{\lambda} \\ &\psi_t^j = \beta V_{t+1}^j \text{ implies } \lambda_t^j \in (0, \overline{\lambda}) \\ &\psi_t^j \geq \beta V_{t+1}^j \text{ implies } \lambda_t^j = 0, \end{aligned} \tag{3}$$

where $\overline{\lambda}$, the cap of capacity from new entrants in each year, is assumed to be the same across energy sources.[13]

The nonstationary oblivious equilibrium is defined as follows. It contains a set of strategies $\{\zeta_t^j, \lambda_t^j\}_{t=0}^{\overline{T}}$ for $j \in \mathcal{J}$ such that in each period $t$,

(a) $\zeta_t^j$ solves the Bellman equation (2), and

(b) $\lambda_t^j$ satisfies free-entry conditions (3).

The algorithm to solve for the equilibrium follows Benkard et al. (2008) closely. I start from a set of initial guesses of $\{\zeta_t^j, \lambda_t^j\}_{t=0}^{\overline{T}}$ for $j \in \mathcal{J}$ and calculate the expected transition path following (1) and profits $\Pi^j(\widetilde{K}_t, z_t), j \in \mathcal{J}$. Next, I solve the Bellman equations (2) by backward induction and check the free-entry conditions (3). I then update the exit strategies $\{\zeta_t^j\}_{t=0}^{\overline{T}}$ based on strategies from two consecutive iterations and update the entry strategies $\{\lambda_t^j\}_{t=0}^{\overline{T}}$ depending on the extent of the violation of the free-entry conditions. An equilibrium is solved if exit strategies $\{\zeta_t^j\}$ from two consecutive iterations are close enough and free-entry conditions are satisfied by $\{\lambda_t^j\}$ for all $j \in \mathcal{J}$.

[13]The inclusion of the cap for capacity from new entrants is motivated by the constraint posed by the interconnection queue. To build a new power plant and connect it to transmission lines, new entrants first need to go through an interconnection queue in which the system operator conducts studies to evaluate their impacts on the grid. Only a few studies can be conducted, which sets a limit on the amount of newly built capacity in each year. Even though it can take on average four years for a generator to get through the interconnection queue in the US, the process is much faster in ERCOT (Clifford, 2023). Therefore, I assume that time to build is only one year.

# 4 Hourly Model of the Wholesale Electricity Market

In this section, I describe the hourly model of competition in the day-ahead wholesale electricity market. Each hourly model corresponds to one period in the entry and exit model. It is associated with a specific value for the profit shifters, $z_t$, and a fixed set of incumbent generators with capacity $K_t$. The model serves two purposes. First, the annual profits are calculated by simulating the model and aggregating hourly profits for a year. Annual profits under model simulations with alternative $(K_t, z_t)$ serve as payoffs in the entry and exit model. Second, carbon emissions and generation costs are evaluated by solving for the hourly model along the transition paths out of the entry and exit model.

The model is designed to capture the main characteristics of the electricity market as presented in Section 2.4. I collapse 24 hours in a day into two model hours: one peak hour and one off-peak hour. Electricity demand and renewable generation are random variables with different distributions at peak hours and off-peak hours. In each hour, dominant coal and natural gas generators first decide whether to operate taking into account start-up costs,[14] and then choose output to maximize profits with an increasing marginal cost and subject to a limited ranges of output.[15]

I model the the start-up decision as a dynamic discrete choice problem in spirit of Rust (1987), similar to Cullen (2011) and Gowrisankaran et al. (2022).[16] I deviate from them in two ways. First, demand and renewable generation enter the market as aggregate shocks. They shape the residual demand faced by coal and natural gas generators, impacting both their operation and profits. Incorporating the aggregate shocks enables me to analyze how shifts in demand and the growth of renewable capacity affect generator profits when integrating the hourly model into the annual model. Second, rather than assuming a constant marginal cost and limiting the output to be either at full capacity or at the minimum requirement, I consider an increasing marginal cost and allow for any generation level ranging from the minimum output requirement to the full capacity, similar to Reguant (2014). My specification allows the marginal cost to increase at different rates for coal and natural gas generators, as suggested in Section 2.4. This difference has implications for how generators' profits would change with price reductions from renewable expansions.[17]

One challenge when solving for the model is the curse of dimensionality from the large number of generators in the market. When deriving the optimal strategy of choosing whether to operate, generators form expectations about future prices by tracking aggregate shocks, including residual demand and natural gas prices, and the number of generators of each type operated in the previous hour. This

[14]Collapsing 24 hours into 2 model hours implicitly assumes that generators commit to keeping the same operation status within each window. This is consistent with data showing that it is rare for a generator to switch its status more than once within a day. It also should be nonproblematic for the counterfactuals because variations in demand and renewable generation occur mainly across days and between peak hours and off-peak hours. The variability within the peak-hour and off-peak-hour time windows is limited.

[15]I do not consider ramping costs — that is, adjustment costs when generators change their output levels rapidly, conditional on operation. Reguant (2014) finds that ramping costs are not significant for coal or CCGT generators under a specification with an increasing marginal cost.

[16]Other studies modelling start-up costs include Reguant (2014) and Jha and Leslie (2021). Reguant (2014) models the role of start-up costs in the context of multi-unit auctions. Jha and Leslie (2021) model start-up costs as mainly fuel costs, which may be appropriate for natural gas generators but is probably inappropriate for large coal generators, where the opportunity costs from equipment damages can be significant.

[17]Both the slope and intercept of marginal cost affect how generators' profits change in response to a price adjustment. Consider a firm with a quadratic marginal cost $C(q) = aq + bq^2$ in a competitive market with the price $p$. The impact of a price change on the generator's profit is given by $\frac{\partial \pi}{\partial p} = \frac{p-a}{2b^2}$. The effect is influenced by both parameters, $a$ and $b$.

creates a large state space with a complicated transition rule. I reduce the state space by solving for a moment-based equilibrium (Ifrach and Weintraub, 2017). Instead of tracking the operational status of all generators, I assume that generators make their start-up decisions based on total output from dominant coal and natural gas generators in the previous hour, $Q_{h-1}$, which as a moment, summarizes the information about how many generators operated in the previous hour.

Next, I lay out the details of different components of the hourly model.

**Electricity Demand** There are an infinite number of hours within one period, $h = 1, 2, 3, \cdots$,[18] with two types $l_h \in \{O, P\}$ alternating, where $O$ stands for off-peak hours and $P$ represents peak hours.

Electricity demand $d_h$ is assumed to be inelastic with respect to electricity price and given by

$$d_h = z_t^d \overline{d}^{l_h} + \varepsilon_h^d,$$

where $\overline{d}^{l_h}$ is the mean electricity demand for hour type $l_h$ and $\varepsilon_h^d$ follows an AR(1) process with hour-type-specific coefficients:

$$\begin{aligned}
\varepsilon_h^d &= \rho^{d,l_h} \varepsilon_{h-1}^d + z_t^d \sigma^{d,l_h} \eta_h^d \\
\eta_h^d &\sim \mathcal{N}(0,1) \\
\eta_h^d &\perp \varepsilon_{h'}^d, \quad h \geq h'.
\end{aligned}$$

In each period the demand shifter $z_t^d$ is fixed, but across periods both means and standard deviations of electricity demand change in both peak and off-peak hours.

**Generation from Wind and Solar** Wind and solar capacities, $K_t^W$ and $K_t^S$, remain fixed within a period. The utilization factor of wind in hour $h$, $\omega_h^W$, is a random variable with similar stochastic structure to electricity demand:

$$\begin{aligned}
\omega_h^W &= \overline{\omega}^{W,l_h} + \varepsilon_h^W \\
\varepsilon_h^W &= \rho^{W,l_h} \varepsilon_{h-1}^W + \sigma^{W,l_h} \eta_h^W \\
\eta_h^W &\sim \mathcal{N}(0,1),
\end{aligned}$$

where $\overline{\omega}^{W,l_h}$ is the mean during hours of type $l_h$, and $\rho^{W,l_h}$ and $\sigma^{W,l_h}$ are hour-type-specific AR(1) coefficients. The utilization factor of solar in hour $h$, $\omega_h^S$, follows

$$\begin{aligned}
\omega_h^S &= \overline{\omega}^{S,l_h} + \sigma^{S,l_h} \varepsilon_h^S \\
\epsilon_h^S &\sim \mathcal{N}(0,1),
\end{aligned}$$

where $\overline{\omega}^{S,l_h}$ is the mean during hours of type $l_h$ and $\sigma^{S,l_h}$ is the hour-type-specific standard deviation of shocks to solar utilization factors. There is almost no persistence in $\varepsilon_h^S$ across hours for solar in the data, therefore, I assume away the AR(1) structure for solar.

[18] Even though the purpose of the hourly model is to collect annual profits, I assume an infinite horizon to avoid non-stationarity. It is computationally difficult to compute models combining both non-stationarity and aggregate shocks.

Given realizations of $\omega_h^W$ and $\omega_h^S$, without curtailment, electricity generation from wind and solar is given by

$$q_h^W = K_t^W \times \omega_h^W$$
$$q_h^S = K_t^S \times \omega_h^S.$$

In the absence of energy storage, electricity supply from renewables in hour $h$ comprises the generation from wind and solar in that hour ($q_h^W$ and $q_h^S$). With zero marginal costs for wind and solar, they meet the electricity demand first, leaving a residual demand for coal and natural gas generators as

$$d_h^r(0) = d_h - (q_t^W + q_t^S),$$

where $d_h^r(0)$ represents the residual demand when energy storage level $z_t^b = 0$. The introduction of energy storage, as measured by a parameter $z_t^b$, smooths the fluctuations of residual demand, $d_h^r(z_t^b)$, across hours. When generation from renewables exceeds demand, I assume that residual demand becomes zero and wind and solar are curtailed proportionally to their output. The details of energy storage and curtailment are given in Appendix II.

**Fuel Prices** I assume that coal prices are fixed at $p^c$ and natural gas prices follow an AR(1) process:

$$p_h^g = z_t^g \mu^g + \rho^g p_{h-1}^g + z_t^g \sigma^g \varepsilon_h^g, \quad \varepsilon_h^g \sim \mathcal{N}(0,1).$$

where $\mu^g$ and $\sigma^g$ are fixed in all periods when nested in the entry and exit model, and the natural gas price shifter, $z_t^g$, changes both the mean and volatility of natural gas prices across periods.

**Electricity Generation by Fringe Generators** Small or infrequently operating generators are classified as fringe generators. I assume that these fringe generators are homogeneous and not constrained by either minimum output requirements or capacity limitations. Similarly to Butters et al. (2021), I assume that the marginal cost of fringe generators has an exponential form:

$$mc^f = \exp\{c_0^f + c_1^f Q_h^f + \sigma^f \eta_h^f\}, \quad \eta_h^f \sim \mathcal{N}(0,1),$$

where $Q_h^f$ is the output from fringe generators in hour $h$, and $\eta_h^f$ is an unobservable that captures any hour-specific market-level shocks that can affect electricity prices. $\eta_h^f$ is assumed to be independent from all other random variables. Given electricity price $p_h$, the output from fringe generators is given by

$$Q_h^f = \frac{\log p_h - c_0^f - \sigma^f \eta_h^f}{c_1^f}.$$

**Electricity Generation from Dominant Generators: Production Decisions** In each hour, dominant generators first decide whether to operate (the start-up decision) taking into account startup costs, and then they decide how much to produce (the production decision). Denote the set of dominant generators that operate in hour $h$ as $\mathcal{G}_h^+$, which is determined by generators' start-up decisions.

Generator $i$ of type $j$ in $\mathcal{G}_h^+$ chooses output to maximize its profit:[19]

$$\pi_{ih} = \max_{q_{ih}} p_h q_{ih} - C^j(q_{ih}; \eta_{ih})$$
$$\underline{q}^j \leq q_{ih} \leq \overline{q}^j,$$

where $q_{ih}$ is the output of generator $i$ in hour $h$. Generator $i$'s output is constrained by the minimum output requirement $\underline{q}^j$ and capacity $\overline{q}^j$. $C^j(q_{ih}; \eta_{ih})$ is the cost of producing $q_{ih}$ and I assume that it has the following functional form:

$$C^j(q_{ih}; \eta_{ih}) = \underbrace{p_h^j \times H^j q_{ih}}_{\text{fuel costs}} + \underbrace{(\mu^j + \sigma^{c,j}\eta_{ih})q_{ih} + \frac{\alpha^j}{2\overline{q}^j}(q_{ih} - \underline{q}^j)_+^2}_{\text{VO\&M costs}}$$
$$\eta_{ih} \sim \mathcal{N}(0,1),$$

where $(q_{ih} - \underline{q}^j)_+ = \max\{q_{ih} - \underline{q}^j, 0\}$. The cost consists two parts. First, fuel costs are the product of fuel price $p_h^j$ (\$/MMBtu) and heat rate $H^j$ (MMBtu/MWh), which measures the fuel efficiency of generators of type $j$. Second, all costs except fuel costs are variable operational and maintenance (O&M) costs. They are assumed to be quadratic; Therefore, generators have a linearly increasing marginal cost. $\mu^j$, associated with fuel cost and a cost shock $\eta_{ih}$, determines the intercept of marginal cost. $\alpha^j$, associated with capacity $\overline{q}^j$, determines the slope of marginal cost. Appendix III derives the optimal output $q_{ih}$ given electricity price $p_h$ and expected profit $E[\pi_{ih}|p_h]$ when $\eta_{ih}$ is integrated out.

**Equilibrium Price** The equilibrium price in each hour is determined by balancing demand and electricity generation from all energy sources:

$$\sum_{i \in \mathcal{G}_h^+} q_{ih}(p_h; \eta_{ih}) + Q_h^f(p_h) = d_h^r(b_t)$$

The operational characteristics of dominant generators and inelastic demand present challenges in establishing equilibrium prices. I will discuss these challenges in two cases:

***Case I: Excess Supply from Dominant Generators***

When the combined minimum output of all dominant generators committed to production surpasses the residual demand ($\sum_{i \in \mathcal{G}_h^+} \underline{q}_{ih} \geq d_h^r(b_t)$), the equilibrium price may not exist because the electricity demand is inelastic to the electricity price. In such a case, I assume that excess electricity supply is freely disposed of, causing the electricity price to drop to its lowest possible value.[20] However, such scenarios are rare because $\mathcal{G}_h^+$ is endogenously determined by generators' equilibrium start-up strategies and generators aim to avoid situations where they would incur losses.

***Case II: Insufficient Supply from Dominant Generators***

Next, consider the case in which the residual demand is not fulfilled when all operating dominant generators produce at their minimum output requirements ($\sum_{i \in \mathcal{G}_h^+} \underline{q}_{ih} < d_h^r(b_t)$). In this case, challenges regarding the existence of equilibrium prices emerge due to the output constraints of dominant generators. Limited by their capacity, it may be insufficient for dominant generators to meet all electricity

[19] Type $j$ is linked to generator $i$. I represent it as $j$ when there is no ambiguity.

[20] I set the lowest value of the electricity price as the intercept of the fringe marginal cost. Setting the lower bound at zero generates almost the same results.

demand. To overcome this, I assume that the representative fringe generator has no capacity constraint. So the fringe can always fill the gap between demand and generation from dominant generators.

A more subtle challenge in establishing the equilibrium price comes from minimum output requirements, which result in multiple flat steps in the aggregate electricity supply curve. I address this issue by incorporating idiosyncratic shocks, $\eta_{ih}$, to the intercept of marginal cost, reducing the length of those plateaus. In any case where the demand realization falls within the middle of a flat step, residual demand is adjusted by curtailing renewable generation to achieve equilibrium.[21]

An alternative method to tackle the challenges associated with establishing equilibrium prices is to consider the possibility of blackouts. However, I implicitly assume away blackouts because of the flexibility of fringe supply. Nonetheless, my model can provide insights into the reliability issues in the electricity market by analyzing electricity prices. In situations where there's inadequate capacity from dominant generators, electricity prices can experience sharp increases.

**Electricity Generation from Dominant Generators: Start-Up Decisions** Before discussing the details of start-up decisions, I lay out the timing assumptions.

- At the beginning of each hour, electricity demand $d_h$, renewable productivity $\omega_h^W, \omega_h^S$, and natural gas price $p_h^G$ are realized.
- Observing the total output from dominant generators in the previous hour ($Q_{h-1}$), the electricity demand ($d_h$), the capacity factor of wind ($\omega_h^W$), the capacity factor of solar ($\omega_h^S$), and the natural gas price ($p_h^G$), each dominant generator decides whether or not to operate, as captured by the indicator variable, $\chi_{ih}$, after observing an idiosyncratic shock associated with each action, $\varepsilon_{ih}^{\chi}$.
- Marginal cost shocks associated with dominant generators, $\eta_{ih}$, and fringe generators, $\eta_h^f$ are realized. Fringe generators and operating dominant generators choose their output and earn profits.
- Electricity is consumed, and the market moves to the next hour.

I focus on the moment-based equilibrium in which generators make start-up decisions using strategies based on states $\{\chi_{ih-1}, l_h, d_h^r, p_h^g, Q_{h-1}\}$. The following Bellman equation characterizes the dynamic programming problem when making start-up decisions:

$$V_i^{l_h}(\chi_{ih-1}, d_h^r, p_h^G, Q_{h-1}) = E_{\varepsilon_{ih}} \max\{\sigma^j \varepsilon_{ih}^{\chi_{ih-1}} + \beta W_0^{j,l_h}(d_h^r, p_h^G, Q_{h-1}), \\ \sigma^j \varepsilon_{ih}^{\chi_{ih-1}} + \Pi^j(d_h^r, p_h^G, Q_{h-1}) - \kappa^j \mathcal{I}\{\chi_{ih-1} = 0\} + \beta W_1^{j,l_h}(d_h^r, p_h^G, Q_{h-1})\}, \tag{4}$$

where $\chi_{ih}$ is an indicator function that takes the value of 1 when a generator operates. $\Pi^j(d_h^r, p_h^G, Q_{h-1})$ is type-$j$ generator's perceived expected profits in hour $h$. $\kappa^j$ is the start-up cost incurred when a generator of type $j$ switches from off to on. $\varepsilon = \{\varepsilon_{ih}^0, \varepsilon_{ih}^1\}$ follow independent type I extreme value distributions with mean 0 and scale parameter $\sigma^j$. $W_0^{j,l_h}$ and $W_1^{j,l_h}$ are choice-specific value functions as in

[21] Each step is associated with at most one generator due to the idiosyncratic shock $\eta_{ih}$. Consequently, only a small margin of curtailment from wind generation is needed to reach an equilibrium. The minimum wind capacity in periods I study is 1.7GW, sufficient for the adjustment.

Rust (1987). They give continuation values associated with operation decisions in hour $h$. Given the distribution assumption for $\varepsilon$, $W_0$ and $W_1$ are given as follows:

$$\begin{aligned}
W_1^{j,l_h}(d_h^r, p_h^g, Q_{h-1}) &= E^{l_{h+1}|l_h}_{d_{h+1}^r, p_{h+1}^g, Q_h} V_i^{l_{h+1}}(1, d_{h+1}^r, p_{h+1}^g, Q_h) \\
&= E^{l_{h+1}|l_h}_{d_{h+1}^r, p_{h+1}^g, Q_h} \sigma^j \log\{\exp\{\frac{\Pi^j(d_{h+1}^r, p_{h+1}^g, Q_h) + \beta W_1^{j,l_{h+1}}(d_{h+1}^r, p_{h+1}^g, Q_h)}{\sigma^j}\} \\
&+ \exp\{\frac{\beta W_0^{j,l_{h+1}}(d_{h+1}^r, p_{h+1}^g, Q_h)}{\sigma^j}\}\}
\end{aligned}$$

$$\begin{aligned}
W_0^{j,l(h)}(d_h^r, p_h^g, Q_{h-1}) &= E^{l_{h+1}|l_h}_{d_{h+1}^r, p_{h+1}^g, Q_h} V_i^{l_{h+1}}(0, d_{h+1}^r, p_{h+1}^g, Q_h) \\
&= E^{l_{h+1}|l_h}_{d_{h+1}^r, p_{h+1}^g, Q_h} \sigma^j \log\{\exp\{\frac{\Pi^j(d_{h+1}^r, p_{h+1}^g, Q_h) - \kappa + \beta W_1^{j,l_{h+1}}(d_{h+1}^r, p_{h+1}^g, Q_h)}{\sigma}\} \\
&+ \exp\{\frac{\beta W_0^{j,l_{h+1}}(d_{h+1}^r, p_{h+1}^g, Q_h)}{\sigma^j}\}\},
\end{aligned}$$

where the expectation is taken over a perceived transition kernel that specifies the perceived distribution of $d_{h+1}^r, p_{h+1}^G, Q_h$ given $d_h^r, p_h^G, Q_{h-1}$ when the market moves from hour type $l_h$ to $l_{h+1}$.

Next, I discuss the perceived transition kernel and the perceived expected profits. One challenge when using the moment-based equilibrium is that the moment $Q_{h-1}$, which summarizes the operation status of all generators, might not follow a Markov process because part of the information is lost when aggregating individual operation status to total output. Following Gowrisankaran et al. (2022) and Barwick et al. (forthcoming), I approximate the transition process of $Q_{h-1}$ by a parametric AR(1) process. Specifically, I assume that the perceived transition rule of $Q_h$, conditional on $d_h^r$ and $p_h^g$, follows a deterministic rule:

$$Q_h = \theta_0^{l_h} + \theta_1^{l_h} d_h^r + \theta_2^{l_h} p_h^g + \theta_3^{l_h} Q_{h-1}, l_h \in \{O, P\}. \tag{5}$$

Though simple, the AR(1) specification is able to capture the effect of residual demand and natural gas prices on dominant generation and, therefore, the electricity price. $Q_{h-1}$ captures the possible state dependence due to the start-up cost.

Given the perceived transition kernel, the perceived single-hour profit of type-$j$ generators is then given by

$$\Pi^j(Q_h^f) = E[E[\pi_{ih}|p_h(Q_h^f; \eta_h^f)]|Q_h^f],$$

where the inner expectation is taken over the perceived transition kernel and the transition of $d_h^r$ (since $Q_h^f = d_h^r - Q_h$), and the outer expectation is taken over $\eta_h^f$.[22]

**Definition of the Moment-Based Equilibrium** A moment-based equilibrium consists of a set of start-up strategies $\chi_{ih}^{l_h}(\chi_{ih-1}, d_h^r, p_h^g, Q_{h-1})$ for generator $i$ of type $j \in \{$coal, small natural gas, large natural gas$\}$ and a set of belief parameters $\theta^{l_h} = \{\theta_0^{l_h}, \theta_1^{l_h}, \theta_2^{l_h}, \theta_3^{l_h}\}$ for $l_h \in \{O, P\}$ such that

(a) $\chi_{ih}^{l_h}(\chi_{ih-1}, d_h^r, p_h^g, Q_{h-1})$ solves the Bellman equation (4)

[22] I calculate the outer expectation using 8th-order Gauss-Hermite quadrature.

(b) $\theta^{l_h}, l_h \in \{O, P\}$ are consistent with simulated data generated from $\chi_{ih}^{l_h}(\chi_{ih-1}, d_h^r, p_h^g, Q_{h-1})$

**Algorithm** I describe the algorithm used to compute the moment-based equilibrium. The algorithm is similar to Ifrach and Weintraub (2017) and Gowrisankaran et al. (2022). I start from a set of candidate belief parameters $\theta^{l_h}, l_h \in \{O, P\}$. Then, I compute the transition matrix of $(d_h^r, p_h^g, Q_h)$ by discretizing the AR(1) process associated with $\theta^{l_h}, l_h \in \{O, P\}$. Next, I solve the start-up strategies $\chi_{ih}^{l_h}(\chi_{ih-1}, d_h^r, p_h^g, Q_{h-1})$ as solutions to the Bellman equation (4). I then forward simulate the start-up decisions and output decisions of all generators in the market and collect $Q_h$ for a large-enough number of hours $H$. Next, I update the belief parameters by estimating regressions of $Q_h$ on $d_h^r, p_h^g$ and $Q_h$ by employing OLS, separately for peak hours and off-peak hours. An equilibrium is achieved if the belief parameters in two consecutive iterations are close enough.

**Annual Outcomes** Having solved for the moment-based equilibrium, I calculate the annual profits of different types of generators as well as total generation costs and carbon emissions. The calculation is a by-product of the forward simulation step in the algorithm solving for the equilibrium.[23]. For a dominant generator $i$, the profit is given by

$$\Pi_t^j = E[\sum_{h=1}^{365\times 2} (p_h q_{ih} - C^j(q_{ih}; \eta_{ih}))\mathcal{H}_h - \kappa^j \mathcal{I}\{\chi_{ih} = 1, \chi_{ih-1} = 0\} + \varepsilon_{ih}^{\chi_{ih}})],$$

where the expectation is taken over different simulation draws of $\{\eta_h^f, \eta_{ih}, \varepsilon_{ih}^{\chi_{ih}}\}$, and $\mathcal{H}_h$, which maps one peak hour to 8 data hours and one off-peak hour to 16 data hours. The profits have four components, revenue, generation costs, start-up costs, and a revenue correction term for the type I extreme value shocks.

The profits of wind and solar are given as follows:

$$\Pi_t^W = \sum_{h=1}^{365\times 2} p_h q_h^W \mathcal{H}_h - C^W$$
$$\Pi_t^S = \sum_{h=1}^{365\times 2} p_h q_h^S \mathcal{H}_h - C^S,$$

where $q_h^W$ and $q_h^S$ are output from wind and solar, and $C^W$ and $C^S$ are annual fixed O&M costs for wind and solar.

Total generation costs include fuel costs, variable O&M costs and start-up costs for dominant generators, annual fixed costs for wind and solar, as well as costs for fringe generation. The costs for the representative fringe generator is

$$\begin{aligned} C_t^{\text{fringe}} &= \sum_{h=1}^{365\times 2} \mathcal{H}_h \int_0^{Q_h^f} \exp\{c_0^f + c_1^f q + \sigma^f \eta_h^f\} dq \\ &= \frac{\exp\{c_0^f + \sigma^f \eta_h^f\}}{c_1^f} (\exp\{c_1^f Q_h^f\} - 1). \end{aligned}$$

[23] I take the average of various outcomes across multiple 730-hour windows and generators of the same type in the forward simulation step of the solution algorithm for the moment-based equilibrium.

Annual carbon emissions from electricity generation of type-$j$ generators are given as follow:

$$Q_t^{j,\text{carbon}} = \sum_{i \in \mathcal{G}_h^+} \tau^j \sum_{h=1}^{365\times 2} q_{ih} \mathcal{H}_h$$

where $\tau^j$ is the emission rate of $CO_2$(tons/MWh) from generators of type $j$. Electricity generation from fringe generators also produce carbon emissions. I assume that fringe generators have the same carbon emission rates as natural gas generators.

# 5 Estimation and Calibration

In Section 5.1, I discuss the identification and estimation of parameters in the hourly model. Then, I present the estimation results and model fits. In Section 5.2, to illustrate the effects of competition between different energy sources, I present the first-order approximation of the profit surface, which is trained by a deep neural network. Finally, in Section 5.3, I discuss how I calibrate parameters in the annual entry and exit model.

## 5.1 Estimation of Generation Costs and Start-up Costs

I apply the hourly model to ERCOT data in 2020. I first collapse the original data across 24 hours in a day into 2 model hours, as detailed in Appendix I. I then conduct the estimation in two steps. First, I estimate distributions of aggregate market variables including electricity demand, wind and solar utilization factors, and natural gas prices. In the second step, I jointly estimate generation costs and start-up costs associated with dominant generators and marginal costs associated with fringe generators via simulated method of moments. The parameters to be estimated in the second step are summarized in $\Xi$:

$$\Xi^{\text{hourly}} = \{ \underbrace{\alpha^j, \mu^j, \sigma^{c,j}}_{\text{generation costs}}, \quad \underbrace{\kappa^j, \sigma^j}_{\text{start-up costs}} \quad , \quad \underbrace{c_0^f, c_1^f, \sigma^f}_{\text{fringe marginal costs}} \quad \}$$

$$j \in \{\text{coal, small natural gas, large natural gas}\}$$

The estimation procedure is nested. In the inner loop, I solve for the moment-based equilibrium, simulate the model for $T$ periods, and calculate moments from the simulated data. In the outer loop, I search for the parameters that best match simulated moments and data moments.

### 5.1.1 Identification

I discuss in this section the identification of cost parameters. Parameters in the O&M costs are identified from the first-order condition of dominant generators' profit-maximization problem. As shown in Appendix III, without output constraints, the utilization factors $q_{ih}^*/\overline{q}^j$ are proportional to electricity prices $p_h$ net of fuel costs $p_h^j H^j$ when a generator is on. By focusing on observations when the output is strictly in between $\underline{q}^j$ and $\overline{q}^j$, the positive correlation between electricity prices and utilization factors identifies $\alpha^j$, and the average and standard deviation of utilization factors help identify $\mu^j$ and $\sigma^{c,j}$.

The identification of start-up costs is similar to Cullen (2011). First, consider generators' start-up decisions without start-up costs and the associated type I extreme value shocks. In this case, the start-up decisions follow a cutoff rule (Rust, 1987): regardless of previous operation status, generators will choose to operate if the expected profits are above zero; otherwise, they are off. However, with start-up costs present, generators remain operating when the expected profits are moderately negative to avoid future start-up costs. Therefore, $\kappa^j$ are identified by the differences in probability of operating when generators have the same expected profits but different operation status in the previous hour. Given that fuel costs account for a substantial share of start-up costs, I parameterize $\kappa^j, j \in \{\text{small natural gas, large natural gas}\}$ as

$$\kappa^j = \kappa_0^j + \kappa_1^j p_h^g.$$

$\kappa_1^j$ is identified by the difference in the probability of operating under various natural gas prices. The scale parameters $\sigma^j$ can be identified by comparing the operational probabilities in the model incorporating those unobserved shocks with the probabilities in a deterministic model. Finally, the marginal cost curve of the representative fringe generator is identified by the correlation between the fringe output and the electricity price.

The moments used in the estimation are (1) the mean and standard deviation of utilization factors across different residual demand realizations when generators operate within nonbinding output constraints; (2) the probability of a generator turning on after being off, across five residual demand realizations; (3) the same probability as in (2), but for generators operated in the previous hour; (4) the probability of a generator turning on after being off, across different natural gas prices; (5) the probability of a generator operating, separately for peak and off-peak hours; (6) electricity prices and total output from different types of generators, separately for peak and off-peak hours.

### 5.1.2 Estimation Results

**Electricity Demand, Renewable Productivity, and Natural Gas Prices** Details for my results are presented in the Appendix. Table A-1 summarizes electricity demand, and wind and solar utilization factors by hour. Despite being collapsed into two hours, they are consistent with the descriptions in Section 2.4. Tables A-2 and A-3 report estimates of hour-specific AR(1) processes for shocks to electricity demand and wind utilization factors. The correlation coefficient between $\eta_h^d$ and $\eta_h^w$ is 0.0485, supporting the assumption that demand shocks $\eta_h^d$ and shocks to wind production $\eta_h^w$ are independent.

Natural gas prices exhibit remarkable persistence, characterized by an AR(1) coefficient of 0.99. The accompanying constant of 0.02 indicates an average natural gas prices of approximately \$2/MMBtu in 2020. The standard deviation of AR(1) residuals is 0.056, corresponding to a volatility of natural gas prices that is at approximately \$0.4/MMBtu. This underscores the substantial fluctuations in natural gas prices.

**Estimate of Cost Parameters** Table 2 reports estimates of cost parameters. The estimates are consistent with the main characteristics in the operation of coal and natural gas generators as discussed in Section 2.4. The slope of marginal costs, which are determined by $\alpha^j$ and capacity $\overline{q}^j$, is $\$0.014/MWh^2$ for natural gas generators, approximately twice as high as for coal ($\$0.0064/MWh^2$). The values of $\alpha^j$ and $\mu^j$ jointly determine O&M costs. At maximum capacity, O&M costs for small natural gas and

coal generators are \$5.63/MWh and \$6.10/MWh, close to the engineering estimates of variable O&M costs in Mann et al. (2017) which are \$4.73/MWh and \$6.33/MWh for natural gas and coal generators respectively.

The estimated start-up cost associated with coal generators is \$0.69 million per start-up, similar to Gowrisankaran et al.'s (2022) estimate of \$0.6 million for the start-up cost for 600MW coal generators. Start-up costs are \$0.03 million for small generators and \$0.09 million for large generators. Those costs are comparable with estimates from Cullen (2011) and Reguant (2014). They are very significant, though much smaller than those for coal generators.

The intercept of fringe generators is estimated to be 2.13. Ignoring shocks to the fringe marginal cost, it sets a lower bound for electricity prices at \$8.4/MWh when there is no fringe generation. When fringe generation increases by 1GW, the marginal costs of fringe generators, and therefore electricity prices, increase by 14.7%.

Table 2: Estimation Results of Cost Parameters

| Parameter | Description | Gas:Small | Gas: Large | Coal |
|---|---|---|---|---|
| Panel A. Dominant Generators | | | | |
| $\alpha^j$ | parameters in the slope of marginal costs (\$/MWh) | 3.531 | 0.562 | 4.727 |
| $\mu^j$ | constant part of marginal costs (\$/MWh) | 5.427 | 9.108 | 5.308 |
| $\sigma^{c,j}$ | standard deviation of marginal cost unobservables (\$/MWh) | 1.287 | 1.132 | 0.447 |
| $\kappa_0^j$ | constant part of startup costs (million \$) | 0.022 | 0.000 | 0.691 |
| $\kappa_1^j$ | slope of startup costs (million \$) | 0.004 | 0.043 | |
| $\sigma^j$ | scale parameters of T1EV shocks (million \$) | 0.014 | 0.024 | 0.078 |
| Panel B. Fringe Generators | | | | |
| $c_0^f$ | intercept of fringe marginal costs | 2.128 | | |
| $c_1^f$ | slope of fringe marginal costs (per GW) | 14.722 | | |
| $\sigma^f$ | standard deviation of fringe marginal costs | 0.1296 | | |

***Notes:*** The table reports estimates of generation costs and start-up cost associated with dominant generators and estimates of marginal costs of fringe generators, based on hourly data in ERCOT in 2020. Standard errors are to be added.

Table A-4 presents profits of different types of generator. Coal generators earn the most annual profits, \$19.73 million. Small natural gas generators are the most profitable per MW because natural gas prices were extremely low in 2020.

Finally, I calibrate annual fixed O&M cost as \$0.035 million/MW (Stehly et al., 2020; Lantz et al., 2016) for on-shore wind and \$0.017 million/MW for distributed solar panels (Walker et al., 2020,Wiser et al., 2020).

### 5.1.3 Model Fit

To evaluate the model's performance, I compare data moments with the simulated moments. The exercise shows that, despite its parsimonious specification and limited heterogeneity, the model adequately captures the main operational characteristics and approximates aggregate market outcomes. Table 3 compares means and standard deviations of electricity prices and outputs from each type of generator in the data and the average in the model simulations, separately at peak and off-peak hours. They align

with each other closely.

Table 3: Electricity Prices and Generation by Type of Generators

| | Off-Peak Hours | | Peak Hours | |
|---|---|---|---|---|
| | Data | Model | Data | Model |
| Electricity Price ($/MWh) | 18.23 | 20.42 | 34.22 | 31.77 |
| | (5.29) | (3.38) | (20.54) | (21.69) |
| Electricity Generation: Small Gas (GWh) | 10.56 | 11.40 | 14.26 | 14.25 |
| | (3.24) | (4.26) | (2.90) | (4.76) |
| Electricity Generation: Large Gas (GWh) | 2.52 | 2.16 | 3.46 | 3.26 |
| | (1.35) | (1.23) | (1.59) | (1.87) |
| Electricity Generation: Coal (GWh) | 7.29 | 6.92 | 9.51 | 9.65 |
| | (1.60) | (2.72) | (2.32) | (3.21) |

***Notes:*** The table provides a comparison of the means and standard deviations (in parentheses) for electricity prices and outputs between the observed data and the averaged results from model simulations. This comparison is presented separately for both peak hours and off-peak hours.

Table A-5 presents means and standard deviations of utilization factors under different realizations of residual demand. They are calculated when generators operate and neither the minimum output requirement nor capacity is binding. The model reflects the positive correlation between electricity generation and residual demand. It fits particularly well under low and moderate residual demand realizations, which account for the majority of hours.

Table 4 shows that the model also predicts well the start-up decisions of generators. Model simulations perfectly match data for the start-up frequencies. For coal and large natural gas generators, it also fits well the difference of operational probabilities at peak and off-peak hours. One caveat is that the model underestimates that difference for small gas generators. Table A-6 shows the operational probabilities under different previous operational statuses, by different realizations of residual demand. The model effectively captures the disparities in the operational probabilities under different previous status, especially when realizations of residual demand are low or moderate. However, it tends to overestimate the probability of continuing to operate in two consecutive hours with high residual demand realizations. Table A-7 also presents the probability of switching from off to on, by different realizations of natural gas prices.

Table 4: Start-up Frequency and Probability of Operation

| | Gas: Small | | Gas: Large | | Coal | |
|---|---|---|---|---|---|---|
| | Data | Model | Data | Model | Data | Model |
| Pr[start up] | 0.10 | 0.11 | 0.08 | 0.08 | 0.01 | 0.01 |
| Pr[on\|off-peak hours] | 0.63 | 0.69 | 0.55 | 0.59 | 0.66 | 0.64 |
| Pr[on\|peak hours] | 0.80 | 0.76 | 0.66 | 0.64 | 0.83 | 0.83 |

***Notes:*** The table presents a comparison between data and model simulations in terms of the probability of start-up — that is, the share of hours when a generator switches from off to on and the probability of operation at off-peak and peak hours. compares between data and simulations the probability of start up, that is the share of hours when a generator switches from off to on, and the probability of being on during off-peak hours and peak hours.

## 5.2 Profit Surfaces Linking the Hourly Model with the Annual Model

To compute annual profits within various states $(K_t, z_t)$ for the annual entry and exit model, it is necessary to solve the hourly model $\overline{T}$ times in each iteration when solving for the nonstationary oblivious equilibrium. This iterative process may require numerous iterations for the model to reach convergence. Although solving the hourly model individually is efficient, the cumulative time required can become quite substantial.

To accelerate the computation of annual profits while preserving the richness of dynamics in the wholesale electricity market, I solve the hourly model across an extensive range of predetermined values for $(K_t, z_t)$, as indicated in Table A-8. It's worth noting that the bounds for each variable are chosen generously to ensure that the capacity of each energy source in all counterfactual scenarios falls within the range of evaluation points. This means that when utilizing the approximated profit surface, no extrapolation is involved. Similarly to Bodéré (2023), I then train a deep neural network to approximate the annual profits.[24]

To understand the impact of states $(K_t, z_t)$ on profitability of various generator types, Table 5 presents the OLS estimates of the profit surface. The dependent variables are annual profits ($ million/GW) for each generator type, while the independent variables are the states $(K_t, z_t)$. Before discussing the economic findings, It's noteworthy that the relatively low R-squares observed with natural gas and coal imply significant nonlinearity in the relationship between annual profits and these states. This underscores the critical necessity of employing a deep neural network to approximate the profit surface.

There are three findings from Table 5. First, there are significant competition effects between any two types of energy source. Importantly, the business stealing effects of renewables on coal are almost twice as large as the effects on natural gas. Second, the increase in natural gas prices reduces profits of natural gas generators and increases profits of all the other generators, especially coal generators. Third, the rise in electricity demand provides coal generators with nearly twice the benefit it offers natural gas, while wind and solar gain less from an increase in demand.

[24] I use an $8 \times 32 \times 32 \times 5$ deep neural network in which there are eight input variables $(K_t, z_t)$ and five output variables ($\Pi^j, j \in$ {small natural gas, large natural gas, coal, wind, solar}.)

Table 5: Profit Surface ($ million/GW): OLS Approximation

| | Small Natural Gas | Large Natural Gas | Coal | Wind | Solar |
|---|---|---|---|---|---|
| $K^{\text{small natural gas}}$(GW) | -1.937*** | -1.781*** | -1.830*** | -0.575*** | -0.325*** |
| | (0.011) | (0.011) | (0.013) | (0.005) | (0.002) |
| $K^{\text{large natural gas}}$(GW) | -2.674*** | -2.760*** | -2.702*** | -0.853*** | -0.454*** |
| | (0.044) | (0.044) | (0.056) | (0.019) | (0.010) |
| $K^{\text{coal}}$(GW) | -1.451*** | -1.441*** | -3.606*** | -1.137*** | -0.597*** |
| | (0.010) | (0.010) | (0.013) | (0.004) | (0.002) |
| $K^{\text{wind}}$(GW) | -0.720*** | -0.704*** | -1.622*** | -0.828*** | -0.366*** |
| | (0.004) | (0.004) | (0.006) | (0.002) | (0.001) |
| $K^{\text{solar}}$(GW) | -0.543*** | -0.524*** | -1.098*** | -0.449*** | -0.345*** |
| | (0.004) | (0.004) | (0.005) | (0.002) | (0.001) |
| Effects of Energy Storage | -18.874*** | -15.525*** | -40.248*** | -0.913*** | -3.239*** |
| | (0.626) | (0.625) | (0.795) | (0.259) | (0.134) |
| Natural Gas Price Shifter | -13.998*** | -10.730*** | 28.329*** | 9.539*** | 5.119*** |
| | (0.119) | (0.119) | (0.151) | (0.051) | (0.026) |
| Demand Shifter | 122.477*** | 117.552*** | 243.441*** | 101.649*** | 55.710*** |
| | (0.725) | (0.725) | (0.921) | (0.307) | (0.159) |
| Constant | 114.015*** | 99.875*** | 58.948*** | 31.972*** | 20.983*** |
| | (1.126) | (1.125) | (1.430) | (0.488) | (0.252) |
| Observations | 340,558 | 340,558 | 340,558 | 371,520 | 371,520 |
| R-squared | 0.288 | 0.265 | 0.476 | 0.580 | 0.601 |

***Notes:*** The table reports OLS estimates of the profit surface. The dependent variable in each column is the profit ($ million/GW) for each type of generator. Independent variables are capacities of each energy source (GW), the effect of energy storage $z_t^b \in [0, 1]$, the electricity demand shifter $z_t^d \in [0.8, 1.6]$ and the natural gas price shifter $z_t^g \in [1, 5]$.

## 5.3 Calibration of Entry Costs and Scrap Values

The parameters to be calibrated[25] in the annual model are summarized in $\Xi^{\text{annual}}$:

$$\Xi^{\text{annual}} = (\underbrace{\bar{\phi}^{\text{coal}}, \bar{\phi}^{\text{natural gas}}}_{\text{mean scrap values}}, \underbrace{\psi^{\text{coal}}, \psi^{\text{natural gas}}}_{\text{entry costs}}, \quad \underbrace{\{I_t^{\text{wind}}, I_t^{\text{solar}}\}_{t=0}^{\overline{T}}}_{\text{installation costs of renewables}} \quad )$$

The calibration takes two steps. First, I focus on entry costs and mean scrap values associated with coal and natural gas generators.[26] Since no dominant natural gas generator retired in my sample, I calibrate the mean scrap value of natural gas using the discounted present value of annual maintenance costs estimated in Elliott (2022).[27] I calibrate the remaining parameters by aligning trends in capacities of coal and natural gas within the data and model simulations. More precisely, I calibrate the entry

[25]Since I only observe one realization of entry or exit probability for each type of energy in each year, I cannot estimate the parameters in the annual model in this nonstationary environment.

[26]I restrict the entry costs per GW to be same for small and large natural gas generators, and in the following analysis, I sum capacities of small and large generators and report the total as natural gas.

[27]Without observing firms' frequently cycling between operating and not operating, scrap values and fixed costs cannot be separately identified. It is common to assume one of them is zero and estimate the other (Collard-Wexler, 2013). I assume that the mean scrap value is the accumulated annual maintenance (fixed) costs in the future if a generator continued staying in the market. Therefore, under the infinite-horizon assumption, the mean scrap value is calculated as the maintenance cost divided by $(1 - \beta)$.

costs of natural gas generators by matching the capacity increase from 2005 to 2020 in the data with that from model predictions. No dominant coal generator in the sample retired before 2015 and coal entry was essentially forbidden because of environmental regulations after 2015.[28] Therefore, for coal generators, I calibrate entry costs by matching the capacity increase from 2005 to 2015 in data and model predictions, and I calibrate the mean scrap value by matching the capacity reduction between 2015 and 2020 in the same manner.

The calibration proceeds as a nested procedure. In the inner loop, I solve capacities of coal and natural gas across years in the nonstationary oblivious equilibrium, assuming that they have perfect foresight about profit shifters $\{z_t\}_{t=0}^{\overline{T}}$, and wind and solar capacities, $\{K_t^{\text{wind}}, K_t^{\text{solar}}\}_{t=0}^{\overline{T}}$. In the outer loop, I search for parameters that best match capacity changes from model predictions with the data. Wind and solar capacities $\{K_t^{\text{wind}}, K_t^{\text{solar}}\}_{t=0}^{\overline{T}}$ combine both data between 2005 and 2020 and authoritative projections from the Department of Energy (2023) and Asmelash and Prakash (2019). Since both historical data and projections are based on the renewable subsidy scheme before 2020, it is appropriate to use them in the calibration procedure; The capacities of wind and solar in the counterfactuals are endogenously determined from the equilibrium in the annual model. Demand and natural gas price shifters are shown in Figure 2. For the effect of energy storage, I assume that $z_t^b = 0$ until 2030, as suggested in Butters et al. (2021), and they increase linearly until $z_{\overline{T}}^b = 1$.[29]

Table 6: Parameters Related to Entry and Exit ($ million/GW)

| | Value | Source |
|---|---|---|
| Panel A. Entry Costs | | |
| Natural Gas | 923.4 | Matching change in natural gas capacity between 2005 and 2020 |
| Coal | 3288.5 | Matching change in coal capacity between 2005 and 2015 |
| Panel B. Mean Scrap values | | |
| Natural Gas | 332.4 | Elliott (2022) |
| Coal | 855.8 | Matching change in coal capacity between 2015 and 2020 |

***Notes:*** The table reports the calibration of entry costs and mean scrap values associated with natural gas and coal generators. The calibration procedure is described in Section 5.3.

Table 6 presents the calibration results for coal and natural gas generators. The calibrated value of coal entry cost is $3,288.5 million/GW, which is in the range of engineering estimates ($1800 million/GW in Schlissel et al. (2008) to $4,500 million/GW in ESFC (2023). The entry cost of natural gas generators is calibrated to be $923.4 million/GW, about one third that of coal. It also aligns with engineering estimates between $780 million/GW and $1,110 million/GW according to the Annual Electric Generator Reports of EIA. The means of scrap values are calibrated as $332 million/GW for natural gas generators and $855 million/GW for coal generators. The scrap values are a combination of saved fixed

[28]The Carbon Pollution Standard for New Plants (Section 111(b)) effectively prohibit the establishment of new coal power plants (Abito et al., 2022). Therefore, I assume that $\psi^{\text{coal}} = \infty$ for coal after 2015.

[29]I experiment with $z_{\overline{T}}^b \in \{0, 0.2, 0.4, 0.6, 0.8, 1\}$. I find that all of these values give similar calibration values for parameters associated with coal and natural gas. But different trajectories yield different entry costs associated with wind and solar, especially after 2030. Therefore, I choose $z_{\overline{T}}^b = 1$, which provides the closest calibration of renewable installation costs when compared with engineering estimates.

operational costs in the future and decommissioning costs,[30] and my calibration for coal suggests that the former outweighs the latter.

In the second step, I calibrate time-varying installation costs associated with wind and solar. Given the equilibrium coal and natural gas capacity trajectories determined in the first step of calibration, I back out entry costs of wind and solar that are consistent with their historical and projected capacities, using free-entry conditions (3).[31] Then I add back subsidies renewables received to obtain calibrations of installation costs for wind and solar in each year.

Figure 4 compares the model-calibrated installation costs with the engineering estimates. They align closely with each other. Initially, the installation costs of wind were about half of those of solar. However, installation costs of solar declined rapidly since 2015 and became lower than wind after 2018.

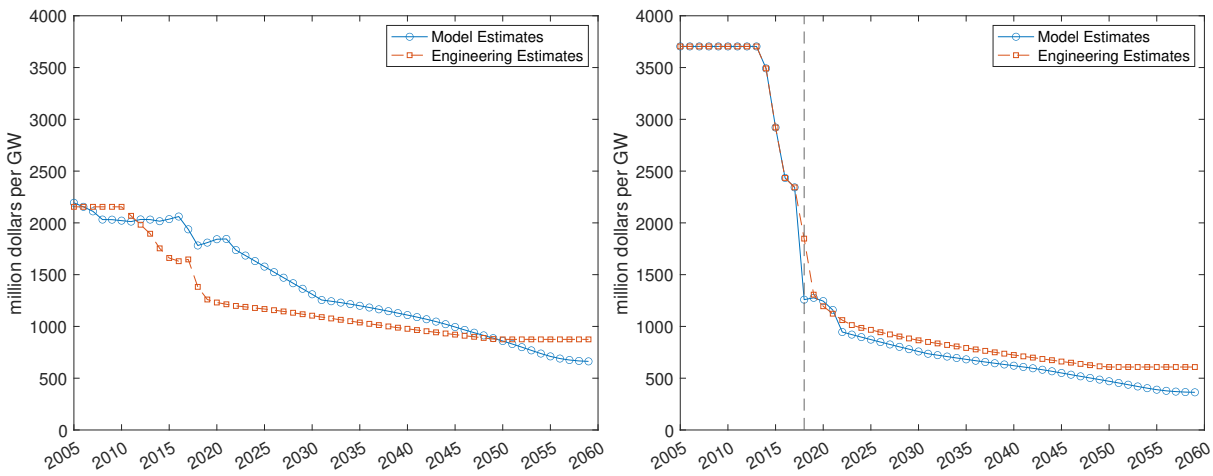


(a) Wind (b) Solar

Figure 4: Installation Costs: Comparison between Model Calibration and Engineering Estimates

*Notes*: The figures compare installation costs of wind and solar from model calibration with those from engineering estimates.

# 6 Counterfactual Results

In this section, I study the equilibrium effects of renewable subsidies and examine how the lengths of subsidies influence those effects. I solve the entry and exit model described in Section 3 to predict average capacity by energy source under counterfactual subsidies that change the time-varying entry costs of renewables. Then I evaluate the carbon emissions and generation costs by solving the hourly model in each year along the transition path.

[30] The decommissioning costs come from utility separation, removal of asbestos and other dangerous materials, managing employees who are no longer able to work at the power plant following its closure, environmental cleanup, and restoring the site to a secure and ecologically sustainable state.

[31] I assume that the capacity cap for new entrants is 10GW for each type of generator, about twice the maximum newly built capacity observed in the data. Therefore, the upper bound is never binding in the calibration. I use the engineering estimates for solar before 2018, when there was no solar entry.

## 6.1 The Effects of Renewable Subsidies

The first counterfactual quantifies the effects of renewable subsidies in place between 2005 and 2020 on carbon emissions, investment, and generation costs by comparing the path with subsidies and the one without them.

Figure 5 plots mean capacities of different energy sources with subsidies between 2005 and 2020 with and without subsidies.[32] Without subsidies in ERCOT, there would be no wind and solar until 2030, at which point installation costs would have decreased sufficiently, paving the way for a rapid expansion of renewable capacities. Coal capacity without subsidies increased by 3.8GW, about 22.6% of maximum coal capacity with subsidies. The increase takes place very early in the transition, even though there is only 0.85GW of wind capacity with subsidies. Consequently, the decreased coal expansion under subsidies cannot be explained by a static model. Instead, subsidies that promote more renewables intensify future competition and diminish the appeal of entering the market. Therefore, fewer coal generators can afford their significant entry costs, leading to a reduction of coal expansion. With natural gas generators' much smaller entry costs, their capacity expands more in the middle of the transition without subsidies, after sufficient retirement of coal generators and before the renewables start to expand.[33]

[32] I assume that after 2020, subsidies phase out linearly until 2030.

[33] The absence of reactions by natural gas generators before 2015 can be attributed to both the expansion of coal and high natural gas prices. Aggressive coal expansion erodes profits of natural gas, and high input prices reduce the benefits that natural gas generators derive from having fewer renewable competitors. Appendix A-3 shows that natural gas capacity will increase without subsidies before 2015 in either of the following two cases. In the first case, I reduce the natural gas price to $4.08/MMBtu whenever it exceeds that limit before 2015. In the second case, the coal expansion is mitigated by a reduction in the capacity cap for new coal generators from 10GW to 5GW.

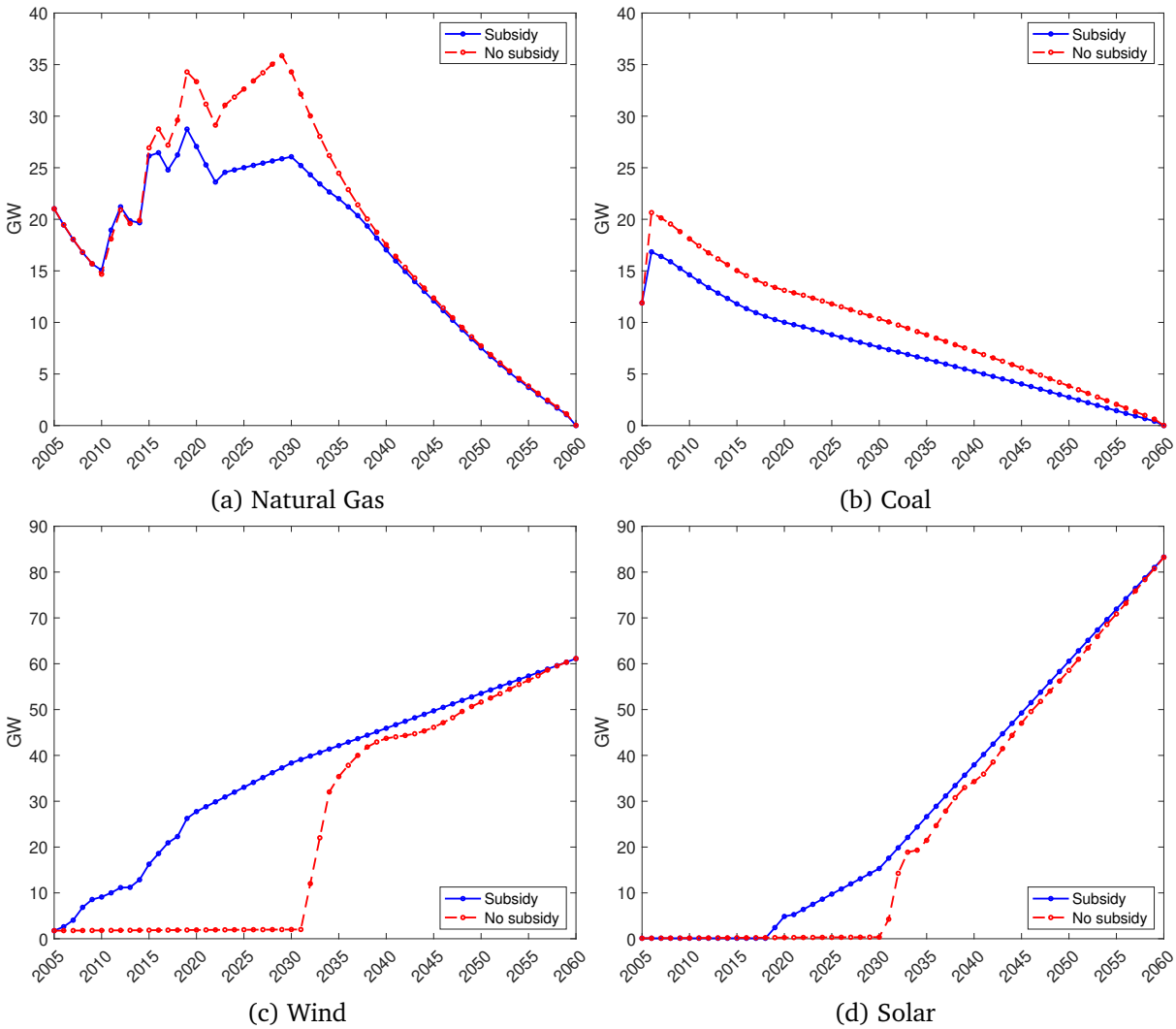


Figure 5: Transition Paths with and without Subsidy

***Notes***: The solid blue lines represent mean capacities of different energy sources with subsidies in place between 2005 and 2020. The dashed red lines are capacity paths of different energy sources when subsidies are removed.

Carbon emissions are affected by generator entry and exit and generator adjustments to their production decisions. Figure 6 displays annual and cumulative carbon emissions since 2005 with and without subsidies between 2005 and 2020 and that without subsidies. Figure 6b shows that renewable subsidies reduce cumulative carbon emissions by 1.71 billion tons through 2060. They reduce environmental costs by \$23.9-\$121.8 billion, evaluated at the social cost of carbon of \$36.6/ton (Carleton et al., 2022) or \$185/ton (Rennert et al., 2022). Figure 6a indicates that the increase in carbon emissions from initial coal expansion persists for multiple decades. I further calculate the differences in carbon emissions from coal generation with and without subsidies. I find that 66% of carbon savings can be explained by the deterred coal expansion.

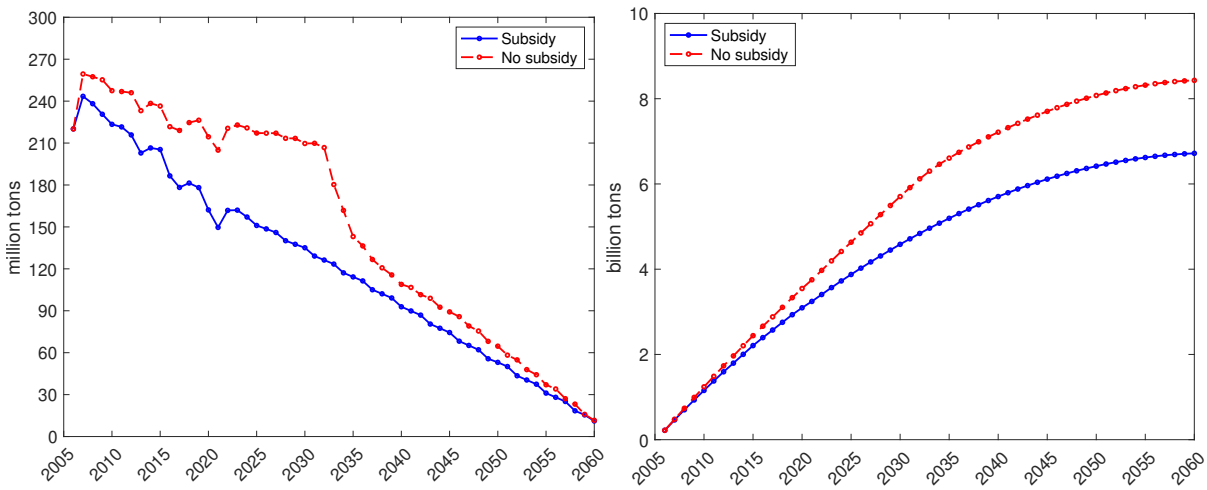


(a) Annual Carbon Emissions

(b) Cumulative Carbon Emissions

Figure 6: Effects of Subsidies on Carbon Emissions

***Notes***: Panel (a) presents carbon emissions in each year and Panel (b) presents cumulative carbon emissions since 2005. The solid blue lines represent outcomes along the transition path with renewable subsidies in place between 2005 and 2020. The dashed red lines represent counterfactuals in which those renewable subsidies were removed.

In addition to considering environmental effects, I consider the effects of subsidies on economic surpluses, including investment and electricity generation costs. Climate policies are often at the heart of political debate partly because the evaluation of environmental benefits is based on the politically contentious social cost of carbon (Hahn and Ritz, 2015). Therefore, it is also useful to examine the effectiveness of renewable subsidies from an economic surplus standpoint. Figure 7 presents cumulative investment and generation costs over the entire simulation horizon. The investment includes installation costs paid by all new entrants net of the mean scrap values of retired generators. Through 2060, renewable subsidies save generation costs by $13.27 billion associated with an increase in investment by $20.09 billion. Subsidies increase investment because the earlier adoption of renewables does not reap the benefits from reduction in installation costs in the future. The generation cost reductions mainly come from less natural gas capacity when there are subsidies. The small distortion for the economic surplus implies that the subsidies can effectively function with a much lower social cost of carbon, $3.99/ton, compared to recent estimates.

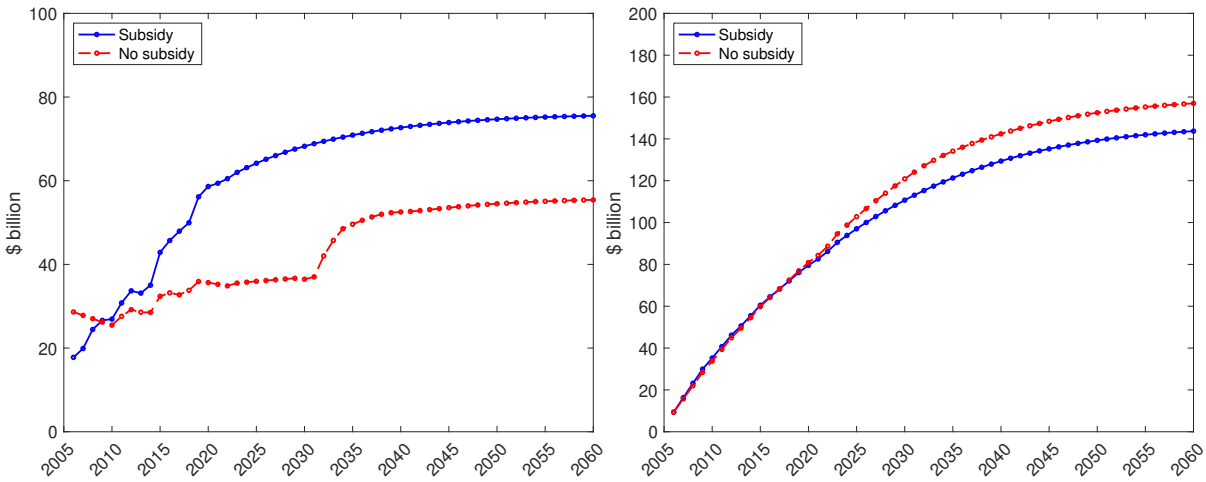


(a) Cumulative Investment Costs (b) Cumulative Generation Costs

Figure 7: Effects of Renewable Subsidies

***Notes***: Panel (a) presents cumulative investment since 2005, and Panel (b) presents cumulative electricity generation costs since 2005. The cumulative investment and generation costs are both calculated as present discount values with a discount rate 0.95. The solid blue lines represent outcomes along transition path with renewable subsidies in place between 2005 and 2020. The dashed red lines represent the counterfactuals in which the subsidies are removed.

## 6.2 The Effects of Different Subsidy Horizons

The time horizon for renewable subsidies is a crucial aspect of policy design, and it presents a significant challenge for policymakers. This challenge is evident in the recurring cycle of subsidy expiration and reauthorization that occurred before 2020. Furthermore, it's underscored by the recent commitment in the IRA 2022 to extend these subsidies for an at least additional 10 years. The uncertainty surrounding the duration of these subsidies highlights the difficulty policymakers encounter when making decisions in this regard. To better understand how different time horizons affect the performance of those subsidies, I study the impacts of different-horizon subsidies on transitional dynamics and carbon emissions.

I simulate the transition paths under alternative subsidy horizons with the generosity of the subsidies fixed at 27$/MWh for PTCs and 30% of installation costs for ITCs. Then, I evaluate the environmental and economic surpluses along those counterfactual transition paths. To illustrate the mechanisms, I display the details of transitional dynamics and their impacts for a short-horizon policy (2005–10), a medium-horizon policy (2005–20, same as Section 6.1 and presented for comparison purposes) and a long-horizon policy (2005–32). I summarize the effects of subsidies with other horizons in Table 7.

Figure 8 presents the expected capacities of different energy sources. Panel 8c and 8d show the trajectories of wind and solar capacities, which are directly affected by the subsidies. Short-horizon and medium-run subsidies do not change the renewable subsidies by 2060, but only the timing when renewables expand. Long-horizon subsidies can impact both investment timing and the resulting wind and solar capacity. This suggests that subsidies with very long horizon will result in wind investment that would never occur throughout the transition without those subsidies. Compared with shorter-horizon subsidies, by 2060, the subsidies between 2005–32 increase wind capacity by 26.6GW and decrease solar capacity by 36.7GW. The difference between wind and solar comes from the diffence in the nature of

PTCs and ITCs. With the uniform nature of PTCs, eligible wind generators can receive the same amount of subsidies regardless of the timing of entry, but with installation costs steadily decreasing, eligible solar generators will receive less subsidies from later investment. Additional wind capacity reduces solar profits, and therefore, reduces solar capacity.

Subsidies with different horizons impact the timing of renewable expansions due to bunching effects. Short-horizon subsidies encourage significant wind capacity growth between 2005 and 2010 because renewables invest earlier to secure their eligibility, which depends on entry before the expiration year. Very-long-horizon subsidies exhibit another form of bunching, where wind generators prefer not to enter the early phase of the transition but cluster in years when the subsidies are about to expire. The reason is that, by investing later, besides subsidies, wind generators can also reap the benefits of exogenous reduction in installation costs.

The direct effects on wind and solar capacities will significantly influence the entry and exit decisions of coal and natural gas generators, as demonstrated in Panel 8b and Panel 8a. Panel 8b reveals a nonlinearity between the subsidy horizon and the effectiveness of driving out coal capacity. A short-horizon subsidy speeds up wind investment and greatly intensifies competition for coal generators in the very near future. The long-horizon subsidy can deter coal entry because, even though the competition will arise from the more distant future, it will be more intense due to the significantly larger wind capacity replacing solar. Solar has a smaller competitive impact on coal compared to wind because it can only produce during the daytime.

Natural gas generators respond differently to changes in renewable capacities compared to coal generators. With short-horizon subsidies, the reduced competition from fewer coal generator almost cancels out the impact of more intensive competition from wind before 2010. Consequently, there is little difference in natural gas capacity before 2015 between short and medium-horizon subsidies. However, long-horizon subsidies incentivize more early natural gas expansion in the transition, with more coal capacity being replaced and less competition from wind between 2005 and 2020. These variations in responses between coal and natural gas generators stem from differences in competition effects in the presence of increased renewable capacity, as well as disparities in entry costs for these generators. For instance, the intense competition resulting from additional wind capacity in 2025-2032, incentivized by very long-horizon subsidies, can deter coal entry as early as 2006 because coal takes many years to recover its high entry costs. In contrast, natural gas can enter between 2005 and 2020 in the long-horizon subsidy path because renewables have a smaller impact on natural gas profits, allowing them to recover their entry costs more quickly due to their lower entry costs.

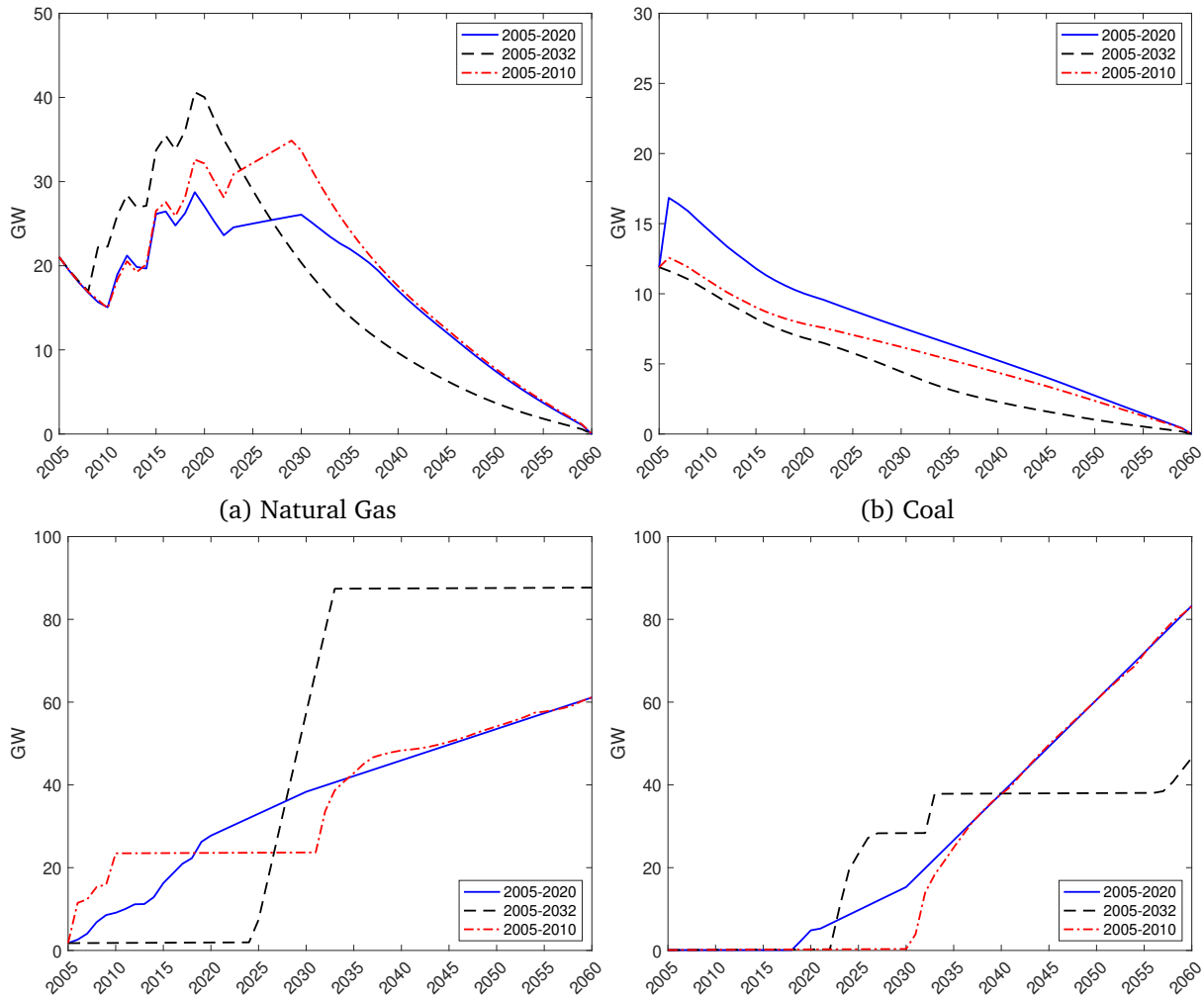


Figure 8: Transition Paths: Alternative Horizons

***Notes***: The figure plots expected capacities of natural gas, coal, wind, and solar between 2005 and 2060 under subsidies with different horizons. The solid blue lines represent the transition path with subsidies in place between 2005 and 2020, as in Figure 5, for ease of comparison. The dash-dotted black lines represent the transition path with subsidies in place between 2005 and 2032. The dashed red lines represent the transition paths under subsidies between 2005 and 2010.

Differences in transitional dynamics induced by different subsidy horizons have implications for both environmental consequences and economic surpluses. Figure 9a compares cumulative carbon emissions since 2005 associated with varying subsidy horizons. First, a short-horizon subsidies have better performances in carbon emissions through the entire transition path than the medium-horizon subsidies actually implemented between 2005 and 2020. This is a combined effect of accelerated wind entry and the deterrence of coal in the initial period of the transition. Second, the effects on cumulative carbon emissions can be heterogeneous across time. The cumulative carbon emissions by 2060 are lowest under the long-horizon subsidies but, the short-horizon subsidies perform the best through 2030. The non-linearity between subsidy horizons and effects on cumulative carbon emissions cautions a careful

design of subsidy horizons and underscores the importance of considering rich dynamics from forward-looking generators.

Turning to the impacts on generation costs displayed in Figure 9b, it reveals a trade-off about the effects of subsidy horizons: the longer horizons deliver more carbon reductions are associated with less reduction in generation costs. The long-horizon subsidies which reduce the most carbon emission by 2060 result in highest generation costs, largely because of the early expansion of high-cost natural gas capacity.

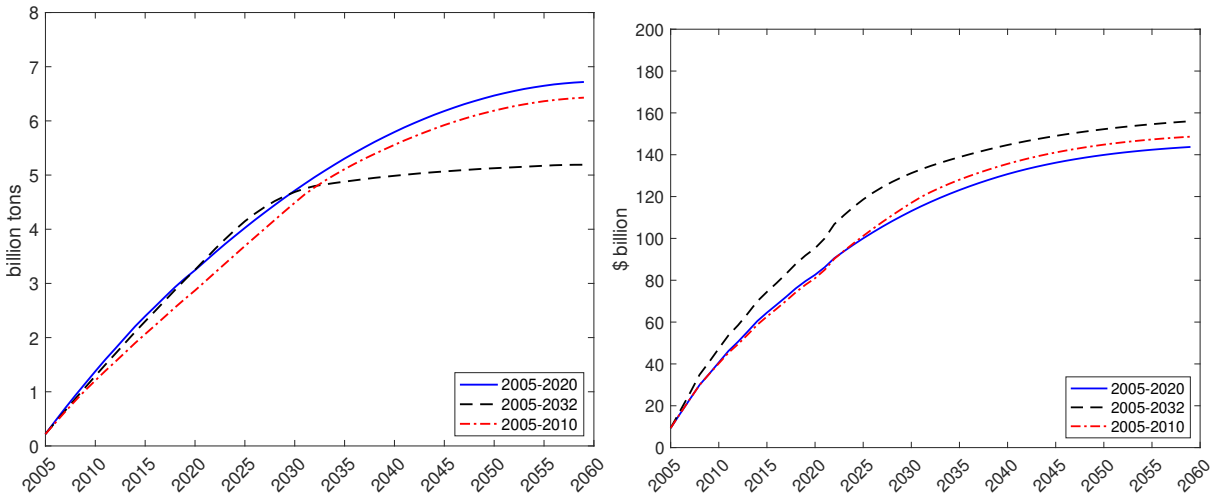


(a) Cumulative Carbon Emissions (b) Cumulative Generation Cost

Figure 9: Effects of Alternative Subsidy Horizons on Carbon Emissions and Generation Costs

***Notes***: Panel (a) presents cumulative carbon emission, and Panel (b) presents present discounted value of generation costs, both since 2005. The solid blue lines represent the transition path with subsidies in place between 2005 and 2020, as in Figure 5, for ease of comparison. The dash-dotted black lines represent the transition path with subsidies in place between 2005 and 2032. The dashed red lines represent the transition paths under subsidies between 2005 and 2010.

To compare the performances from subsidies with varying horizons, Table 7 reports the reductions in environmental costs between transition paths with different subsidies and the unsubsidized path. The environmental costs are calculated in terms of their present discounted values, using the same discount rate applied by generators in the entry and exit model. They are evaluated at two different social cost of carbon values: \$36.6/ton and \$185/ton. The table demonstrates that 5-year short-horizon subsidies can effectively reduce carbon emissions and save on environmental costs in a timely manner. They can achieve similar present discounted savings in environmental costs as subsidies with durations of ten years or longer, including those extending beyond twenty years. The non-linearity between the subsidy time horizon and environmental cost reduction emphasizes the importance of a carefully designed time horizon. For instance, among the subsidies under consideration, 22-year subsidies result in the most substantial environmental cost reduction, while subsidies that are 3 years shorter than those perform poorly in reducing carbon emissions. The reason behind this is that the 19-year subsidies delay wind investment, but the additional wind capacity is not sufficient to deter coal entry in the initial transition process.

Table 7 also reports the present discounted values of changes in total investment, tax expenditure,

private investment (investment net of tax expenditure), and generation costs when compared with the unsubsidized path. As expected, subsidies with longer horizons put heavier burden on tax payers. A five-year subsidies can save $2.7 billion tax expenditure than a twenty-two-year subsidies with comparable environmental cost savings. The appeal of short-term subsidies lies in their minimal tax burden and their comparable impact on carbon reduction. Tax burden plays a crucial role in shaping public perception and, consequently, in determining the feasibility of such policies, as highlighted by Christian Gollier and Mar Reguant in Blanchard et al. (2021) that "the visibility of the levy to the payers (consumers or the taxpayers) often shapes attitudes much more than the actual amount of money levied upon them to avoid the emission of one ton of CO2." Table 7 also shows a quadratic relationship between subsidy horizons and investment. The longer-horizon subsidies have lower investment in present discounted term because wind investment delays due to the bunching effect. The reduction in generation costs also exhibit a similar quadratic relationship because of not only delayed wind investment but the resulting more natural gas capacity in the early phase of the transition process.[34]

Table 7: Environmental and Economic Impacts of Subsidy Horizons ($ billion)

| | Environmental Cost (-) | Investment (+) | Tax Expenditure (+) | Private Investment (+) | Generation Cost (-) |
|---|---|---|---|---|---|
| 1 year | [19.2,97.6] | 3.7 | 0.5 | 3.2 | 3.1 |
| 5 years | [32.4,165.2] | 12.3 | 1.0 | 11.3 | 8.4 |
| 10 years | [32.6,166.0] | 16.0 | 1.4 | 14.6 | 10.3 |
| 15 years | [18.9,96.3] | 18.6 | 1.8 | 16.9 | 11.9 |
| 16 years | [23.9,121.8] | 20.1 | 1.5 | 18.6 | 13.3 |
| 17 years | [31.9,162.7] | 16.3 | 1.8 | 14.5 | 12.2 |
| 19 years | [15.9,80.8] | 15.7 | 2.3 | 13.5 | 11.2 |
| 22 years | [35.6,181.5] | 7.8 | 3.7 | 4.1 | 4.9 |
| 25 years | [35.3,179.7] | 5.4 | 4.2 | 1.2 | 3.2 |
| 28 years | [34.0,173.2] | 1.8 | 4.7 | -2.9 | 1.0 |

***Notes***: The table compares environmental cost from carbon emissions (evaluated at either $36.6/ton or $185/ton), investment, tax expenditure, private investment (investment net of tax expenditure) and generation costs, between the transition path with varying subsidy horizons and the unsubsidized path. All terms are in their present discounted values, with discount rate same as generators, 0.95.

# 7 Conclusion

This paper studies the effects of renewable subsidies on carbon emissions, total investment, and generation costs. The subsidies target clean energy sources, but those effects are realized through equilibrium responses of coal and natural gas generators via both changes in production decisions and entry and exit. To simulate how subsidies change the transition path, I build a nonstationary model of generator entry and exit at the annual level. To determine annual profits, I nest the model with a secondary dynamic model of the wholesale electricity market in which all generators compete to produce electricity every hour and where coal and natural gas generators face start-up costs. I apply the models to ERCOT, the electricity grid covering the majority of Texas. I estimate the hourly model using detailed hourly data

[34]While some may prioritize environmental costs, given the fat-tailed uncertainty of climate change, as evidenced by the substantial estimates of the social cost of carbon Weitzman (2011), it remains valuable to analyze the economic surplus resulting from investment and generation costs. This is because the funds saved can be redirected toward other pollution reduction efforts, further contributing to carbon emissions reduction. I calculate the opportunity cost of reducing carbon emissions using the increased economic surplus (as the difference between additional investment costs and the reduced generation costs) at a marginal abatement cost of $12/ton, the average of the range of marginal abatement costs estimated by Meng (2017). I find that five-year subsidies still stand out among subsidies shorter than twenty years by reducing environmental costs by $20.36 billion.

and calibrate the annual model so that it is consistent with observed and projected capacity changes in ERCOT.

I find that renewable subsidies can reduce cumulative carbon emissions by 1.7 billion tons through 2060 and that 66% of the effect comes from reduced coal expansion in the initial year of the transition. The deterrence of coal expansion comes before renewables enter at large scale because the lasting presence of renewable subsidies increases future competition and therefore shifts the expectations of coal generators. This cannot be captured by a model that does not incorporate forward-looking perspective of generators. In addition to their environmental impacts, subsidies reduce the costs of generating electricity by $13.3 billion with an extra investment of $20.1 billion, which implies that the renewable subsidies can work with a social cost of carbon as low as $3.99/ton.

To understand how the policy maker can design the horizon of subsidies to achieve better performance by leveraging the dynamic mechanism, I examine the effects of subsidies with varying durations. The analysis reveals a nonlinear relationship between subsidy durations and carbon reductions. A Short-horizon subsidy can accelerate more wind investment early in the transition and deter the entry of dirty coal generators. Though a long-enough-horizon subsidy can postpone wind investment, it can facilitate coal-to-gas switch because additional wind capacity incurred by the subsidy have stronger competition effects on coal than natural gas. Both of the short-horizon and long-horizon subsidies can outperform the medium-horizon one, including the one actually implemented between 2005–20.

There are two important future directions, building upon the framework presented in this paper. First, given the nature of intermittent generation, more renewable capacity can increase the volatility of the electricity grid. Lacking energy storage, the grid requires generators with lower start-up costs to cycle between on and off multiple times in a day. Low-start-up-cost, high-marginal-cost open-cycle natural gas generators, therefore, can complement renewables. It is therefore important to consider the role of such generators in grid stability in the energy-transition process. Second, through more detailed modeling of battery operations in the hourly model and incorporating the investment costs of the batteries, the framework can be extended to study the equilibrium responses of fossil fuel generators to the development of energy storage, which is important to evaluate the environmental benefits from investing in energy-storage technologies.

# References


Jose Miguel Abito. Measuring the welfare gains from optimal incentive regulation. *The Review of Economic Studies*, 87(5):2019–2048, 2020.

Jose Miguel Abito, Christopher R Knittel, Konstantinos Metaxoglou, and André Trindade. The role of output reallocation and investment in coordinating environmental markets. *International Journal of Industrial Organization*, 83:102843, 2022.

E Asmelash and G Prakash. Future of solar photovoltaic: Deployment, investment, technology, grid integration and socio-economic aspects. *International Renewable Energy Agency, Abu Dhabi*, 2019.

Panle Jia Barwick, Myrto Kalouptsidi, and Nahim Bin Zahur. Industrial policy implementation: Empirical evidence from china's shipbuilding industry. *The Review of Economic Studies*, forthcoming.

C Lanier Benkard. A dynamic analysis of the market for wide-bodied commercial aircraft. *The Review of Economic Studies*, 71(3):581–611, 2004.

CL Benkard, Przemyslaw Jeziorski, B Van Roy, GY Weintraub, et al. Nonstationary oblivious equilibrium. Technical report, 2008.

John Bistline, Neil Mehrotra, and Catherine Wolfram. Economic implications of the climate provisions of the inflation reduction act. Technical report, National Bureau of Economic Research, 2023.

Olivier Blanchard, Jean Tirole, Christian Gollier, Mar Reguant, Dani Rodrik, Stefanie Stantcheva, Axel Boersch-Supan, Claudia Diehl, Carol Propper, Philippe Aghion, et al. Major future economic challenges-june 2021. 2021.

Pierre Bodéré. Dynamic spatial competition in early education: An equilibrium analysis of the preschool market in pennsylvania. Technical report, Working paper, 2023.

Bryan Bollinger and Kenneth Gillingham. Learning-by-doing in solar photovoltaic installations. *Available at SSRN 2342406*, 2019.

Severin Borenstein and Ryan Kellogg. Carbon pricing, clean electricity standards, and clean electricity subsidies on the path to zero emissions. *Environmental and Energy Policy and the Economy*, 4(1): 125–176, 2023.

Severin Borenstein, James B Bushnell, and Frank A Wolak. Measuring market inefficiencies in california's restructured wholesale electricity market. *American Economic Review*, 92(5):1376–1405, 2002.

James Bushnell and Kevin Novan. Setting with the sun: The impacts of renewable energy on conventional generation. *Journal of the Association of Environmental and Resource Economists*, 8(4):759–796, 2021.

James B Bushnell, Erin T Mansur, and Celeste Saravia. Vertical arrangements, market structure, and competition: An analysis of restructured us electricity markets. *American Economic Review*, 98(1): 237–66, 2008.

R Andrew Butters, Jackson Dorsey, and Gautam Gowrisankaran. Soaking up the sun: Battery investment, renewable energy, and market equilibrium. Technical report, National Bureau of Economic Research, 2021.

El Hadi Caoui. Estimating the costs of standardization: Evidence from the movie industry. *The Review of Economic Studies*, 90(2):597–633, 2023.

Tamma Carleton, Amir Jina, Michael Delgado, Michael Greenstone, Trevor Houser, Solomon Hsiang, Andrew Hultgren, Robert E Kopp, Kelly E McCusker, Ishan Nath, et al. Valuing the global mortality consequences of climate change accounting for adaptation costs and benefits. *The Quarterly Journal of Economics*, 137(4):2037–2105, 2022.

Aditya Choukulkar. *Don't Mess with Texas: Getting the Lone Star State to Net-Zero by 2050*. University of Colorado Boulder, 2022.

Catherine Clifford. Wind and solar power generators wait in yearslong lines to put clean electricity on the grid, then face huge interconnection fees they can't afford, 2023. URL https://www.cnbc.com/2023/04/06/outdated-us-energy-grid-tons-of-clean-energy-stuck-waiting-in-line.html.

Allan Collard-Wexler. Demand fluctuations in the ready-mix concrete industry. *Econometrica*, 81(3): 1003–1037, 2013.

Thomas R Covert and Richard L Sweeney. Winds of change: Estimating learning by doing without cost or input data. Technical report, Working paper, 2022.

Joseph Cullen. Measuring the environmental benefits of wind-generated electricity. *American Economic Journal: Economic Policy*, 5(4):107–133, 2013.

Joseph A Cullen. Dynamic response to environmental regulation in the electricity industry. 2011.

Joseph A Cullen and Stanley S Reynolds. Market dynamics and investment in the electricity sector. *International Journal of Industrial Organization*, 89:102954, 2023.

Department of Energy. Map: Projected growth of the wind industry from now until 2050, 2023. URL https://www.energy.gov/map-projected-growth-wind-industry-now-until-2050.

EIA. Average cost of wholesale u.s. natural gas in 2022 highest since 2008, 2023a. URL https://www.eia.gov/todayinenergy/detail.php?id=55119#.

EIA. Federal financial interventions and subsidies in energy in fiscal years 2016–2022. Technical report, 2023b.

Thomas Eisenberg. Regulatory distortions and capacity investment: The case of china's coal power industry. Technical report, Mimeo, 2020.

Jonathan T Elliott. Investment, emissions, and reliability in electricity markets. Technical report, Working Paper, 2022.

ESFC. Coal-fired power plant construction costs, 2023. URL https://esfccompany.com/en/articles/thermal-energy/coal-fired-power-plant-construction-costs/.

Natalia Fabra. A primer on capacity mechanisms. *Energy Economics*, 75:323–335, 2018.

Harrison Fell and Daniel T Kaffine. The fall of coal: Joint impacts of fuel prices and renewables on generation and emissions. *American Economic Journal: Economic Policy*, 10(2):90–116, 2018.

Meredith Fowlie. Allocating emissions permits in cap-and-trade programs: Theory and evidence. *University of California, Berkeley*, 2010.

Meredith Fowlie, Mar Reguant, and Stephen P Ryan. Market-based emissions regulation and industry dynamics. *Journal of Political Economy*, 124(1):249–302, 2016.

Todd D Gerarden. Demanding innovation: The impact of consumer subsidies on solar panel production costs. *Management Science*, 2023.

Kenneth Gillingham, Marten Ovaere, and Stephanie M Weber. Carbon policy and the emissions implications of electric vehicles. Technical report, National Bureau of Economic Research, 2021.

Luis E Gonzales, Koichiro Ito, and Mar Reguant. The investment effects of market integration: Evidence from renewable energy expansion in chile. 2023.

Gautam Gowrisankaran, Stanley S Reynolds, and Mario Samano. Intermittency and the value of renewable energy. *Journal of Political Economy*, 124(4):1187–1234, 2016.

Gautam Gowrisankaran, Ashley Langer, and Wendan Zhang. Policy uncertainty in the market for coal electricity: The case of air toxics standards. Technical report, National Bureau of Economic Research, 2022.

Gautam Gowrisankaran, Ashley Langer, and Mar Reguant. Energy transitions in regulated markets. Technical report, Working Paper, 2023.

Robert W Hahn and Robert A Ritz. Does the social cost of carbon matter? evidence from us policy. *The Journal of Legal Studies*, 44(1):229–248, 2015.

Stephen P Holland, Erin T Mansur, and Andrew J Yates. Decarbonization and electrification in the long run. Technical report, National Bureau of Economic Research, 2022.

J Huetteman, J Tafoya, T Johnson, and J Schreifels. Epa-eia power sector data crosswalk, 2021.

Bar Ifrach and Gabriel Y Weintraub. A framework for dynamic oligopoly in concentrated industries. *The Review of Economic Studies*, 84(3):1106–1150, 2017.

IREA Irena. Future of wind: Deployment, investment, technology, grid integration and socio-economic aspects. *Abu Dhabii*, 2019.

Jihye Jeon. Learning and investment under demand uncertainty in container shipping. *The RAND Journal of Economics*, 53(1):226–259, 2022.

Akshaya Jha and Gordon Leslie. Start-up costs and market power: Lessons from the renewable energy transition. *Available at SSRN 3603627*, 2021.

Sarah Johnston, Yifei Liu, and Chenyu Yang. An empirical analysis of the us generator interconnection policy. 2022.

Daniel T Kaffine, Brannin J McBee, and Jozef Lieskovsky. Emissions savings from wind power generation in texas. *The Energy Journal*, 34(1), 2013.

Omer Karaduman. Economics of grid-scale energy storage. *Job market paper*, 2020.

Ömer Karaduman. Large scale wind power investment's impact on wholesale electricity markets. 2021.

Seth D Kirshenberg. *Examination of Federal Financial Assistance in the Renewable Energy Market: Implications and Opportunities for Commercial Deployment of Small Modular Reactors*. Scully Capital, 2018.

Eric Lantz, Benjamin Sigrin, Michael Gleason, Robert Preus, and Ian Baring-Gould. Assessing the future of distributed wind: opportunities for behind-the-meter projects. Technical report, National Renewable Energy Lab.(NREL), Golden, CO (United States), 2016.

Joshua Linn and Kristen McCormack. The roles of energy markets and environmental regulation in reducing coal-fired plant profits and electricity sector emissions. *The RAND journal of economics*, 50 (4):733–767, 2019.

Neal Mann, Chen-Hao Tsai, Gürcan Gülen, Erich Schneider, Pedro Cuevas, Jim Dyer, John Butler, T Zhang, R Baldick, T Deetjen, et al. Capacity expansion and dispatch modeling: Model documentation and results for ercot scenarios. *The Full Cost of Electricity. The University of Texas at Austin Energy Institute*, 2017.

Erin T Mansur. Measuring welfare in restructured electricity markets. *The Review of Economics and Statistics*, 90(2):369–386, 2008.

Kyle C Meng. Using a free permit rule to forecast the marginal abatement cost of proposed climate policy. *American Economic Review*, 107(3):748–784, 2017.

Kevin Novan. Valuing the wind: renewable energy policies and air pollution avoided. *American Economic Journal: Economic Policy*, 7(3):291–326, 2015.

Dana Olson and Bent Erik Bakken. Utility-scale solar pv: From big to biggest. *Hentet*, 10:2020, 2019.

Karen Palmer, Anthony Paul, Matt Woerman, and Daniel C Steinberg. Federal policies for renewable electricity: Impacts and interactions. *Energy Policy*, 39(7):3975–3991, 2011.

Mar Reguant. Complementary bidding mechanisms and startup costs in electricity markets. *The Review of Economic Studies*, 81(4):1708–1742, 2014.

Kevin Rennert, Frank Errickson, Brian C Prest, Lisa Rennels, Richard G Newell, William Pizer, Cora Kingdon, Jordan Wingenroth, Roger Cooke, Bryan Parthum, et al. Comprehensive evidence implies a higher social cost of co2. *Nature*, 610(7933):687–692, 2022.

Edward S Rubin, Inês ML Azevedo, Paulina Jaramillo, and Sonia Yeh. A review of learning rates for electricity supply technologies. *Energy Policy*, 86:198–218, 2015.

John Rust. Optimal replacement of gmc bus engines: An empirical model of harold zurcher. *Econometrica: Journal of the Econometric Society*, pages 999–1033, 1987.

Stephen P Ryan. The costs of environmental regulation in a concentrated industry. *Econometrica*, 80(3): 1019–1061, 2012.

David Schlissel, Allison Smith, and Rachel Wilson. Coal-fired power plant construction costs. *Synapse Energy Economics Inc*, 2008.

Tyler Stehly, Philipp Beiter, and Patrick Duffy. 2019 cost of wind energy review. Technical report, National Renewable Energy Lab.(NREL), Golden, CO (United States), 2020.

James H Stock and Daniel N Stuart. Robust decarbonization of the us power sector: Policy options. Technical report, National Bureau of Economic Research, 2021.

Nicholas Vreugdenhil. Booms, busts, and mismatch in capital markets: Evidence from the offshore oil and gas industry. Technical report, Technical report. Arizona State University, 2020.

H Walker, Eric Lockhart, Jal Desai, Kristen Ardani, Geoff Klise, Olga Lavrova, Tom Tansy, Jessie Deot, Bob Fox, and Anil Pochiraju. Model of operation-and-maintenance costs for photovoltaic systems. Technical report, National Renewable Energy Lab.(NREL), Golden, CO (United States), 2020.

Gabriel Y Weintraub, C Lanier Benkard, and Benjamin Van Roy. Markov perfect industry dynamics with many firms. *Econometrica*, 76(6):1375–1411, 2008.

Gabriel Y Weintraub, C Lanier Benkard, and Benjamin Van Roy. Computational methods for oblivious equilibrium. *Operations research*, 58(4-part-2):1247–1265, 2010.

Martin L Weitzman. Fat-tailed uncertainty in the economics of catastrophic climate change. *Review of Environmental Economics and Policy*, 2011.

Ryan H Wiser, Mark Bolinger, and Joachim Seel. Benchmarking utility-scale pv operational expenses and project lifetimes: results from a survey of us solar industry professionals. Technical report, Lawrence Berkeley National Lab.(LBNL), Berkeley, CA (United States), 2020.

Frank A Wolak. Quantifying the supply-side benefits from forward contracting in wholesale electricity markets. *Journal of Applied Econometrics*, 22(7):1179–1209, 2007.

**APPENDICES FOR ONLINE PUBLICATION**

# I Details in Data Preparation for Estimation

The initial dataset comprises data collected at an hourly frequency throughout a given day. Nonetheless, the model is confined to representing only two hours: a single peak hour and an individual off-peak hour. To facilitate the alignment of the data with the model, I've delineated the peak hour as a time window spanning from 1:00 PM to 8:00 PM, while the off-peak hour encompasses the period from 9:00 PM to 12:00 AM of the subsequent day. By calculating averages within these designated time intervals, I condense electricity demand, electricity prices, renewable output, and electricity generation from each generator into the representation of two model hours.

The process of condensing the on and off statuses of generators presents more complexity, mainly due to the potential occurrence of generator start-ups or shutdowns in the middle of a time window. However, the majority of instances reveal consistent generator statuses, making it feasible to mirror these statuses from the original data. In nearly all cases, if a generator does change its status, it does so only once within a single time window. I define a generator's status by two scenarios.

In scenarios where a generator exhibit an on(off) state in both the preceding and subsequent hours, yet manifest a status transition within the current time window, I infer the generator to be off(on) for the present hour. Otherwise, I compute the proportion of hours in which the generator is on or off within the time window. This proportion guides the determination of a generator's status: if the share of on-hours exceeds that of off-hours, the generator's status is considered on; otherwise, it is categorized as off.

# II Energy Storage and Curtailment from Renewables in the Hourly Model

Instead of modelling the charging and discharging behaviors of energy storage as in Butters et al. (2021), I model the consequences of their behaviors as stabilizing residual demand for coal and natural gas generators, following Karaduman (2020). Specifically, I denote $z_t^b \in [0,1]$ as a measure of the extent that residual demand is stabilized by energy storage and the residual demand with energy storage $z_t^b$ as $d_h^r(z_t^b)$. Without energy storage, the residual demand is $d_h^r(0) = d_h - (q_h^W + q_h^S)$. With full energy storage, I assume there is no variation in residual demand and $d_h^r(1) = E[d_h] - E[q_h^W + q_h^S]$. With $z_t^b \in (0,1)$, the residual demand $d_h^r(z_t^b)$ is a convex combination of $d_h^r(0)$ and $d_h^r(1)$

$$d_h^r(z_t^b) = (1 - z_t^b) \times d_h^r(0) + z_t^b \times d_h^r(1).$$

When electricity generation from wind and solar exceeds electricity demand in hour $h$, that is $d_h^r(z_t^b) < 0$, I assume that they will be curtailed proportional to their output respectively in that hour. Specifically,

$$Q_h^{\text{curtailment}} = -d_h^r(z_t^b) \times \mathcal{I}\{d_h^r(z_t^b) < 0\}$$

$$q_h^W = K_t^W \omega_h^W - Q_h^{\text{curtailment}} \frac{K_t^W \omega_h^W}{K_h^W \omega_h^W + K_h^S \omega_h^S}$$
$$q_h^S = K_t^S \omega_h^S - Q_h^{\text{curtailment}} \frac{K_t^S \omega_h^S}{K_h^W \omega_h^W + K_h^S \omega_h^S}$$

# III Optimal Output and Expected Profits of Dominant Generators

Conditional on operating, given electricity price $p_h$, the interior solution of a dominant generator's profit maximization problem is given by

$$q_{ih}^* = \frac{p_h - (p_h^j H^j + \mu^j + \sigma^{c,j}\eta_{ih})}{\alpha^j} \overline{q}^j + \underline{q}^j$$

Therefore, subject to the production constraint $[\underline{q}^j, \overline{q}^j]$, the optimal output is given by

$$q_{ih} = \begin{cases} q_{ih}^* & \eta_{ih} \in (\underline{\eta}_{ih}, \overline{\eta}_{ih}) \\ \overline{q}^j & \eta_{ih} < \underline{\eta}_{ih} \\ \underline{q}^j & \eta_{ih} > \overline{\eta}_{ih} \end{cases}$$

where

$$\overline{\eta}_{ih} = \frac{p_h - p_h^j H^j}{\sigma^{c,j}}$$
$$\underline{\eta}_{ih} = \frac{p_h - p_h^j H^j - \alpha^j \frac{\overline{q}^j - \underline{q}^j}{\overline{q}^j}}{\sigma^{c,j}}$$

Integrating out idiosyncratic shocks $\eta_{ih}$, the expected profits given $p_h$ is given by [35]

$$\begin{aligned} E[\pi_{ih}|p_h] = & (\frac{(p_h - p_h^j H^j - \mu^j)^2}{2\alpha^j} \overline{q}^j + (p_h - p_h^j H^j - \mu^j)\underline{q}^j)(\Phi(\overline{\eta}_{it}) - \Phi(\underline{\eta}_{ih})) \\ & - \sigma^{c,j}(\frac{(p_h - p_h^j H^j - \mu^j)}{\alpha^j} \overline{q}^j + \underline{q}^j)(\phi(\underline{\eta}_{ih}) - \phi(\overline{\eta}_{it})) \\ & + \frac{(\sigma^{c,j})^2}{2\alpha^j} \overline{q}^j (\Phi(\overline{\eta}_{it}) - \Phi(\underline{\eta}_{ih}) + \underline{\eta}_{ih}\phi(\underline{\eta}_{ih}) - \overline{\eta}_{it}\phi(\overline{\eta}_{it})) \\ & + ((p_h - p_h^j H^j - \mu^j)\overline{q}^j - \frac{\alpha^j}{2\overline{q}^j}(\overline{q}^j - \underline{q}^j)^2)\Phi(\underline{\eta}_{ih}) \\ & + \sigma^{c,j}\overline{q}^j \phi(\underline{\eta}_{ih}) \\ & + (p_h - p_h^j H^j - \mu^j)\underline{q}^j (1 - \Phi(\overline{\eta}_{ih})) \\ & - \sigma^{c,j}\underline{q}^j \phi(\overline{\eta}_{ih}) \end{aligned}$$

[35] I use the fact that if $\eta \sim \mathcal{TRN}(0, 1, a, b)$, then

$$E[\eta] = \frac{\phi(a) - \phi(b)}{\Phi(b) - \Phi(a)}$$

and

$$E[\eta^2] = 1 + \frac{a\phi(a) - b\phi(b)}{\Phi(b) - \Phi(a)}$$

# IV Figures

## IV.1 ERCOT Operates an Isolated Grid

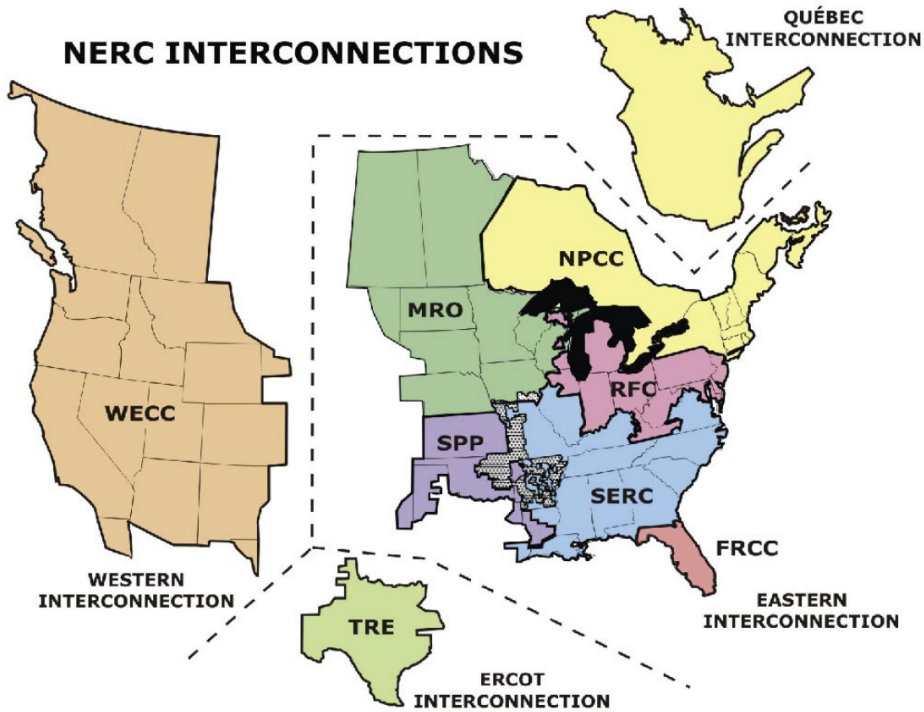


Figure A-1: ERCOT Territory

## IV.2 Calibration of Installation Costs under Alternative $z_T^b$

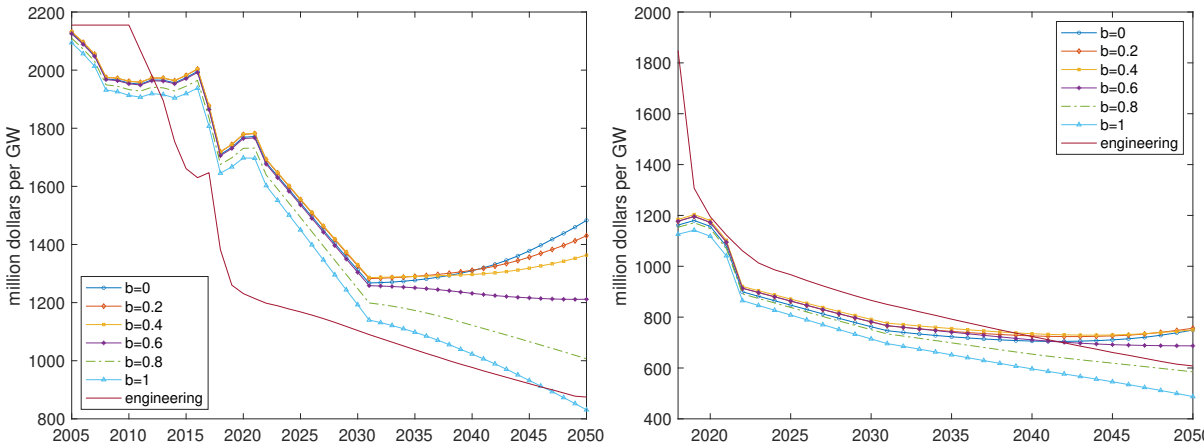


(a) Wind Installation Costs

(b) Solar Installation Costs

Figure A-2: Comparison of Renewable Installation Costs under Alternative Energy Storage Trajectories

*Notes*: The figure compares calibration of wind and solar installation costs under alternative trajectories of energy storage. I assume that the effects of energy storage remain zero until 2030 and start to increase linearly. For other assumptions and details about the calibration procedure, see Section 5.3.

## IV.3 Additional Counterfactuals when Renewable Subsidies were Removed

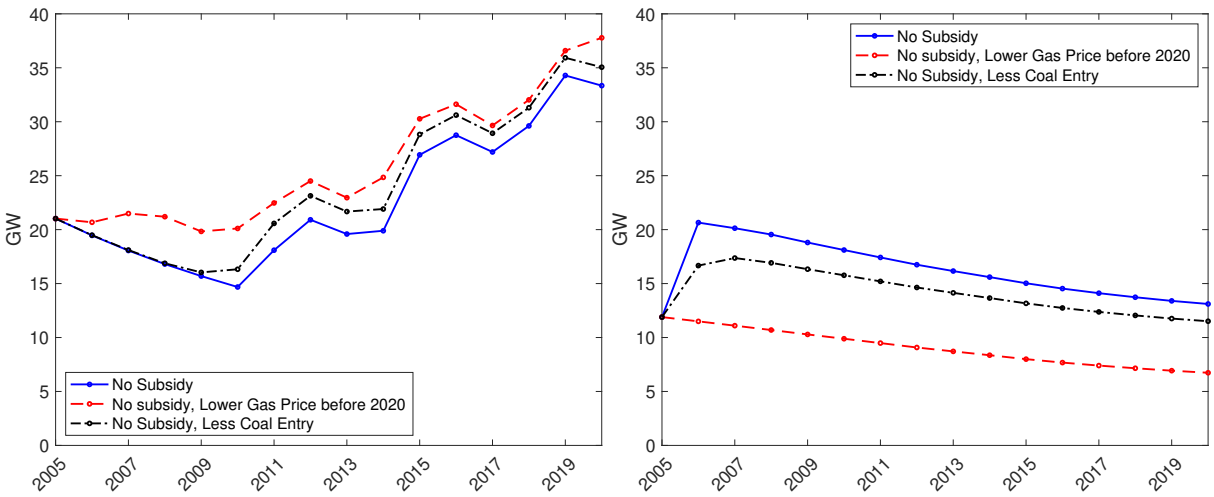


(a) Natural Gas (b) Coal

Figure A-3: Additional Counterfactuals when Subsidies were Removed

*Notes*: The figures provide additional counterfactuals when renewable subsidies were removed to examine why natural gas capacity remains the same as with subsidies before 2015 in Figure 5. The blue solid line represents the natural gas and coal capacity without subsidies, same as Figure 5. The red dash lines represent the natural gas and coal capacities without subsidies when natural gas prices are imposed to be below $4.08 before 2015. The black dash-dot lines represent counterfactual capacities without subsidies when the maximum newly built capacity for coal is reduced from 10GW to 5GW so that coal can only enter less aggressively.

# V Additional Tables

Table A-1: Summary Statistics by Hours (GWh)

| | Off-peak Hours | | Peak Hours | |
|---|---|---|---|---|
| | Mean | SD | Mean | SD |
| $d_h$ | 37.21 | 5.38 | 45.13 | 10.06 |
| $\omega_h^W$ | 0.383 | 0.154 | 0.306 | 0.166 |
| $\omega_h^S$ | 0.105 | 0.050 | 0.404 | 0.180 |

***Notes:*** The calculation relies on the hourly electricity demand and the utilization factors of wind and solar in ERCOT for the year 2020. Peak hours, which include those between 1:00 PM and 8:00 PM, are consolidated as one, while the remaining hours are grouped as off-peak hours. Subsequently, the average demand and utilization factors are computed for both peak and off-peak hours on a daily basis. Finally, summary statistics are derived from these averaged values.

Table A-2: Estimates of Demand Shock Process (GWh)

| VARIABLES | (1) AR(1) | (2) Off-peak hours | (3) Peak hours |
|---|---|---|---|
| $\rho^d$ | 0.710*** | 0.463*** | 1.577*** |
| | (0.026) | (0.014) | (0.053) |
| Observations | 731 | 365 | 366 |
| Adjusted R-squared | 0.504 | 0.750 | 0.710 |
| $\sigma^d$ | 5.67 | 2.69 | 5.41 |

***Notes:*** Table reports the estimates of demand shock process. Demand shock is the deviation of electricity demand to its mean, by two types of hours. Column (1) group all hours and estimate an AR(1) model, illustrating that the electricity demand is a stationary process overall. Column (2) and (3) estimate two AR(1) model separately for peak hours and off-peak hours. $\sigma^d$ is calculated as the standard deviation of AR(1) residuals.

Table A-3: Wind Productivity Process

| VARIABLES | (1) AR(1) | (2) Off-peak hours | (3) Peak hours |
|---|---|---|---|
| $\rho^w$ | 0.632*** | 0.545*** | 0.732*** |
| | (0.029) | (0.040) | (0.041) |
| Observations | 731 | 365 | 366 |
| Adjusted R-squared | 0.398 | 0.341 | 0.461 |
| $\sigma^w$ | 0.124 | 0.122 | 0.125 |

***Notes:*** Table reports the estimates of wind utilization factor process. Wind utilization factor is the ratio of wind generation and capacity, by two types of hours. Column (1) group all hours and estimate an AR(1) model, illustrating that the wind utilization factor is a stationary process overall. Column (2) and (3) estimate two AR(1) model separately for peak hours and off-peak hours. $\sigma^w$ is calculated as the standard deviation of AR(1) residuals.

Table A-4: Decomposition of Profits, by Type of Generators ($ million)

| | Gas: Small | Gas: Large | Coal |
|---|---|---|---|
| Revenue | 37.45 | 45.99 | 99.71 |
| Generation Costs | 28.90 | 36.79 | 79.78 |
| Static Profits | 8.55 | 9.21 | 19.93 |
| Start-up Costs | 2.38 | 4.75 | 3.90 |
| Unobservables | 4.21 | 6.07 | 3.70 |
| Profits | 10.38 | 10.52 | 19.73 |

***Notes:*** The table reports different components of profits by types of generators, evaluated at the estimated parameters. For the details of computation, see section 4.

Table A-5: Utilization Factors, by Residual Demand (GWh)

| | Gas: Small | | Gas: Large | | Coal | |
|---|---|---|---|---|---|---|
| | Data | Model | Data | Model | Data | Model |
| Panel. A Mean | | | | | | |
| $E[q\|d_h^r < 17.3]$ | 0.80 | 0.80 | 0.59 | 0.64 | 0.55 | 0.54 |
| $E[q\|17.3 \leq d_h^r < 26.2]$ | 0.85 | 0.84 | 0.73 | 0.71 | 0.65 | 0.64 |
| $E[q\|26.2 \leq d_h^r < 35.2]$ | 0.88 | 0.87 | 0.82 | 0.76 | 0.72 | 0.70 |
| $E[q\|35.2 \leq d_h^r < 44.1]$ | 0.90 | 0.90 | 0.86 | 0.82 | 0.81 | 0.85 |
| $E[q\|d_h^r \geq 44.1]$ | 0.93 | 1.00 | 0.93 | 0.90 | 0.92 | 1.00 |
| Panel.B Standard Deviation | | | | | | |
| $SD[q\|d_h^r < 17.3]$ | 0.10 | 0.11 | 0.06 | 0.03 | 0.21 | 0.11 |
| $SD[q\|17.3 \leq d_h^r < 26.2]$ | 0.10 | 0.12 | 0.15 | 0.14 | 0.21 | 0.16 |
| $SD[q\|26.2 \leq d_h^r < 35.2]$ | 0.09 | 0.11 | 0.12 | 0.15 | 0.21 | 0.17 |
| $SD[q\|35.2 \leq d_h^r < 44.1]$ | 0.08 | 0.11 | 0.10 | 0.15 | 0.17 | 0.12 |
| $SD[q\|d_h^r \geq 44.1]$ | 0.06 | 0.03 | 0.10 | 0.14 | 0.09 | 0.00 |

***Notes:*** The table reports means and standard deviations of utilization factors, conditional on different realizations of residual demand(GWh). For both data and simulations, I restrict observations when generators are on, and neither minimum output requirement nor capacity is not binding.

Table A-6: Operation Probabilities, by Residual Demand (GWh)

| | Gas: Small | | Gas: Large | | Coal | |
|---|---|---|---|---|---|---|
| | Data | Model | Data | Model | Data | Model |
| Panel.A Conditional on Not Operating in Previous Hour | | | | | | |
| $d_h^r < 1.73$ | 0.10 | 0.16 | 0.05 | 0.05 | | |
| $d_h^r \geq 1.73, d_h^r < 2.62$ | 0.22 | 0.29 | 0.09 | 0.11 | | |
| $d_h^r \geq 2.62, d_h^r < 3.52$ | 0.35 | 0.49 | 0.28 | 0.24 | 0.05 | 0.03 |
| $d_h^r \geq 3.52, d_h^r < 4.41$ | 0.66 | 0.78 | 0.37 | 0.53 | | |
| $d_h^r \geq 4.41$ | 0.82 | 0.96 | 0.66 | 0.88 | 0.21 | 0.33 |
| Panel.B Conditional on Operating in Previous Hour | | | | | | |
| $d_h^r < 1.73$ | 0.63 | 0.62 | 0.58 | 0.61 | | |
| $d_h^r \geq 1.73, d_h^r < 2.62$ | 0.76 | 0.78 | 0.73 | 0.78 | | |
| $d_h^r \geq 2.62, d_h^r < 3.52$ | 0.89 | 0.88 | 0.90 | 0.91 | 0.99 | 0.99 |
| $d_h^r \geq 3.52, d_h^r < 4.41$ | 0.95 | 0.96 | 0.97 | 0.98 | | |
| $d_h^r \geq 4.41$ | 1.00 | 1.00 | 0.99 | 1.00 | 0.99 | 0.99 |

***Notes:*** The table reports the probability of being on, depending on whether generators are on or off in the previous hour. They are calculated under different realizations of residual demand (GWh). For natural gas generators, the realizations of residual demand are consolidated into five groups and for coal generators, they are grouped into two categories based on whether they are above 44.1 GWh or not.

Table A-7: Probability of Switching from Off to On, by Natural Gas Prices ($/MMBtu)

| | Small Natural Gas | | Large Natural Gas | | Coal | |
|---|---|---|---|---|---|---|
| | Data | Model | Data | Model | Data | Model |
| $p_h^G < 2.4$ | 0.39 | 0.38 | 0.22 | 0.21 | 0.05 | 0.03 |
| $p_h^G > 2.4$ | 0.28 | 0.35 | 0.14 | 0.15 | 0.07 | 0.13 |

***Notes:*** The table reports the probability of switching from off to on, by different realizations of natural gas prices. They are categorized into two groups based on whether natural gas prices are above $2.4/MMBtu or not.

Table A-8: Pre-specified Points of $(K_t, z_t)$ to Solve the Hourly Model

| Parameters | Grid Points |
|---|---|
| Number of Small Gas Generators | 1 30 60 90 120 160 200 240 |
| Number of Large Gas Generators | 1 10 20 30 |
| Number of Coal Generators | 1 10 20 30 40 80 |
| Wind Capacity (GW) | 10 20 40 60 100 150 |
| Solar Capacity (GW) | 1 20 40 60 100 150 |
| effects of energy storage | 0, 0.3, 0.6, 0.9 |
| natural gas price shifter | 1 2 5 |
| demand shifter | 0.8 1 1.2 1.4 1.6 |

*Notes:* The table reports grid points of pre-specified $(K_t, z_t)$ that are used to solve the hourly model and collect annual profits. Note that for small natural gas, large natural gas and coal, instead of directly specifying capacities, I specify the number of generators in each type and then convert them to capacities. The collected annual profits are then used as input to train a deep neural networks to obtain a reliable but computationally fast profit function that serves as payoff in the annual entry/exit model.